NOTE TO USERS

Page(s) missing in number only; text follows. Page(s) were scanned as received.

vi

This reproduction is the best copy available.

UMI®

A Mathematical Approach to Axon Formation in a Network of Signaling Molecules for N2a Cells

by

Majid Bani-Yaghoub

A thesis submitted to

the Faculty of Graduate Studies and Research

in partial fulfillment of

the requirements for the degree of

Master of Science

School of Mathematics and Statistics

Ottawa-Carleton Institute of Mathematics and Statistics

Carleton University

Ottawa, Ontario, Canada

May, 2006

Your file Votre référence
ISBN: 978-0-494-16490-7
Our file Notre référence
ISBN: 978-0-494-16490-7

Abstract

A mathematical model consisting of two reaction-diffusion subsystems is proposed to investigate the effects of Retinoic Acid(RA) and activated Notch1 on axon formation in N2a cells. The subsystems of the model are compelled by the external signals corresponding to activated Notch and RA utilized in the experiment. The subsystems are perturbed by an interaction between RA and Notch signaling pathways hypothesized in the model. On the basis of Turing Theory, the conditions for the existence of symmetry breaking instabilities for axon formation are established and compared for perturbed and unperturbed subsystems. Under some conditions, small perturbations to the system do not change the qualitative behavior of the system. Numerical simulations are presented for Turing instabilities in the presence of Turing, Hopf and saddle-node bifurcations. The theoretical outcomes of this study are explored via laboratory experimentations.

To My wife, Grace

Acknowledgements

I would like to thank my supervisor Dr. David E. Amundsen for his time and patience and for giving me the opportunity to work in the field of mathematical biology. I would also like to thank my brother Dr. Mahmud Bani-Yaghoub for his care, support and guidance in my life and for the biological experiments performed in this study. I want to thank my wife for being supportive and encouraging me to continue my studies. This work would have been worthless and impossible without her corrections to my poor English and her will to type almost all of the pages. I am so grateful to my parents who have been continuously helping me to achieve my goals in life. God bless both of them!

Contents

List of Figures

Chapter 1

Introduction

1.1 What is Biomathematics?

The word biomathematics was used for the first time by Dr. William M. Feldman in 1923. Biomathematics or mathematical biology is an essential tool in several areas of biology and medicine such as population genetics, biomedical imaging, cellular neurobiology, epidemiology and ecology. It plays an important role in understanding many areas of biology and medicine. Biomathematics has grown at an astonishing rate and has established itself as a major discipline in the biomedical sciences. At the present time we are witnessing the increasing integration of biomathematics into academic programs at universities around the world.

Biomathematics is an interdisciplinary field of academic study which aims at modeling natural, biological processes using mathematical techniques and tools. It has both practical and theoretical applications in biological research. Biomathematics differs in various aspects from the field of biostatistics. A major difference between biomathematics and biostatistics is that biomathematics is the study of biological systems through the construction and analysis of models while biostatistics

is the design of hypothesis tests and data analysis in a biological context.

The present work is a mathematical approach to one of the central issues in cellular neurobiology and developmental biology. No previous knowledge of biology is assumed of the reader. I briefly describe the biological background to understand the problem whenever it is necessary. There is also a glossary of biological terms used in this study.

In the present work a mathematical model is employed to study the effects of signaling molecules and chemicals on neuronal differentiation and axon formation. To answer the main questions encountered in this project, I will use some mathematical tools such as perturbation techniques, numerical analysis, bifurcation and linear stability analysis. This study is based on a mathematical theory of biological pattern formation and cell differentiation initiated by British mathematician, Alan Turing. He wrote his seminal paper "The Chemical Basis of Morphogenesis" in 1952 [48] in which he showed that a system of chemicals could evolve spontaneously into a spatial pattern. In the next section I will talk about his theory in more detail.

1.2 Turing Theory

In 1950, Alan Turing started work on a new mathematical theory of morphogenesis. After two years of working on his theory, he demonstrated that pattern formation may take place if some conditions in a system of non-linear equations (describing the kinetics of two chemicals) are satisfied. He hypothesized that biological pattern formation is the result of a competition between two chemicals with different diffusion rates. The chemical that diffuses faster is called the "inhibitor" while the other is called the "activator". In the absence of diffusion, the two chemicals tend to a linearly stable uniform steady state, while in the presence of diffusion the activator

and the inhibitor destabilize the uniform steady state and as a consequence, pattern formation takes place. It is well known that simple reaction-diffusion systems can display very rich pattern formation behavior. What Turing proposed was a mechanism for the development of spatial patterns such as animal coat patterns. J.D. Murray ([29],p.76) provides a good example which is very useful to understanding Turing mechanism:

> *Consider a field of dry grass in which there is a large number of grasshoppers which can generate a lot of moisture by sweating if they get warm. Now suppose the grass is set alight at some point and a flame front starts to propagate. We can think of the grasshopper as an inhibitor and the fire as an activator. If there were no moisture to quench the flames the fire would simply spread over the whole field which would result in a uniform charred area. Suppose, however, that when the grasshoppers get warm enough they can generate enough moisture to dampen the grass so that when the flames reach such a pre-moistened area the grass will not burn. The scenario for spatial pattern is then as follows. The fire starts to spread—it is one of the 'reactants,' the activator, with a 'diffusion' coefficient D_F say. When the grasshoppers, the inhibitor 'reactant', ahead of the flame front feel it coming they move quickly well ahead of it; that is, they have a 'diffusion' coefficient, D_G say, which is much larger than D_F. The grasshoppers then sweat profusely and generate enough moisture to prevent the fire spreading into the moistened area. In this way the charred area is restricted to a finite domain which depends on the 'diffusion' coefficients of the reactants—fire and grasshoppers—and various 'reaction' parameters. If, instead of a single initial fire, there were*

a random scattering of them we can see how this process would result in a final spatially heterogeneous steady state distribution of charred and uncharred regions in the field and a spatial distribution of grasshoppers, since around each fire the above scenario would take place.

The problem with Turing Theory was that the existence of chemical spatial patterns as predicted by his mathematical formulation could not be confirmed experimentally for over forty years. Then in 1990 Patrick De Kepper's group confirmed for the first time the existence of Turing patterns in an experiment [13]. The observation of Turing patterns initiated a renewed interest in Turing pattern formation. Turing Theory is applicable to many branches of biology, particularly developmental and cell biology. Turing demonstrated that chemicals can react and diffuse in such a way that spatial patterns of concentration are established and as a consequence of this, the fate of a cell is determined.

In order to explain more about the Turing mechanism, let us begin by seeing how reaction-diffusion equations arise from simple ideas involving conservation laws. The use of reaction-diffusion equations often follows from simple time and space dependent models whenever there is a general balance law. For modeling the dispersive behavior of concentrations (e.g. of chemicals) or populations (e.g. of cells or animals), in a continuum approach, density functions are employed to describe the distribution of basic particles.

Let $c(\vec{r},t) : \Omega \times \mathbb{R}^+ \rightarrow \mathbb{R}$, where $\Omega \subseteq \mathbb{R}^n$, be the particle density function or concentration. Let $Q(\vec{x},t,..)$ be the net creation of particles at $\vec{r} \in \Omega$ at time t (e.g. the rate of production (birth rate) per unit volume minus the rate of removal (death rate) per unit volume). Let $\mathbb{J}(\vec{r},t,..)$ be the flux density such that for any unit vector $\vec{n} \in \mathbb{R}^n$, the scalar product $\vec{\mathbb{J}} \cdot \vec{n}$ is the net rate at which particles cross a

unit area in a plane perpendicular to $\vec{n}$ (positive in the $\vec{n}$ direction). Now for any regular subset $B \subseteq \Omega$

$$E = \int_B c \, dr \tag{1.2.1}$$

denotes the population mass in B. Here dr is written for the volume increment, $dr_1 dr_2 ... dr_n$ when $\vec{r} = (r_1, r_2, ... r_n)^T$ in Cartesian coordinates. Assume that the rate of change of this mass (i.e. $\frac{dE}{dt}$) is due to particle creation or degradation inside B and the inflow and outflow of particles through the boundary ∂B. That is,

$$\frac{d}{dt} \int_B c \, dr = - \int_{\partial B} \vec{\mathbb{J}} \cdot \vec{n} \, dA + \int_B Q \, dr, \tag{1.2.2}$$

where $\vec{n}$ denotes the outward-oriented normal to B on ∂B. Assuming the underlying fields are smooth (i.e. $\vec{\mathbb{J}} \in C^1$), then apply the divergence theorem to the second integral in (1.2.2) to obtain

$$\int_B c_t \, dr = \int_B \left[-\nabla \cdot \vec{\mathbb{J}} + Q \right] \, dr. \tag{1.2.3}$$

But B was arbitrary in Ω, hence

$$c_t = -\nabla \cdot \vec{\mathbb{J}} + Q, \text{ on } \Omega \times \mathbb{R} \tag{1.2.4}$$

According to Fick's Law, the flux $\vec{\mathbb{J}}$ is proportional to the gradient in the density. Thus

$$\vec{\mathbb{J}} = -d \nabla c. \tag{1.2.5}$$

The constant d is called diffusivity. The minus sign indicates that particles are transported from high to low densities. Using Fick's Law, (1.2.4) becomes a reaction-

diffusion equation,

$$c_t = Q(\vec{r}, t, c) + d\nabla^2 c. \tag{1.2.6}$$

In a system of reaction-diffusion equations for k different chemical (or morphogens), the governing equations can be written in the form

$$\frac{\partial \vec{c}}{\partial t} = f(\vec{c}) + D\nabla^2 \vec{c} \tag{1.2.7}$$

where $\vec{c}\ (r,t) = (c_1, c_2, ...c_k)^T$ is the vector of chemical concentrations at position r and time t, f represents the reaction kinetics and D is the diagonal matrix of positive diffusion constants. By Turing Theory, a necessary condition for pattern formation (and cell differentiation) is that the homogeneous steady state must be linearly stable in the absence of diffusion ($D = 0$). We can find the eigenvalues of the linearized system $J(f)_{\vec{c}_o}$, the Jacobian matrix of f evaluated at the steady state. Necessary conditions for linear stability can be derived in terms of eigenvalues such that $Re(\lambda_i) < 0$ for all i.

Sufficient conditions for Turing patterns are that the homogeneous steady state must be unstable to spatial perturbations (i.e. presence of diffusion must destabilize the steady state). In particular the eigenvalue equation becomes the determinant

$$\left|J(f)_{c_o} - \lambda I - Dk^2\right| = 0, \tag{1.2.8}$$

where k corresponds to a spatial Fourier mode (more details are provided in Chapter 3). We can find the eigenvalues which are unstable, namely those with positive real part (i.e. $Re(\lambda_i) > 0$ for some i) and thus sufficient conditions can be derived from that. A reaction-diffusion system exhibits diffusion-driven instability (Turing instability) if the homogeneous steady state of (1.2.7) is stable to small perturbations

in the absence of diffusion but unstable to spatial perturbations when diffusion is present. Conditions derived from $Re(\lambda_i) < 0$ for all i when $k = 0$ and $Re(\lambda_i) > 0$ for some $k > 0$ for some i guarantee the existence of Turing instability. The related steady state is called a Turing steady state. This means that cells with concentration values of chemicals close to the corresponding values components of a Turing steady state may differentiate to a certain type of cell (e.g. neurons) while cells with different concentration values may remain undifferentiated. In the next section we will learn about some extensions and applications of Turing Theory. Also, we will learn about the difficulties of the Turing mechanism in some areas of biology.

1.3 Extensions and applications of Turing Theory

The Turing mechanism has been applied to a large number of biological situations, particularly animal coat patterns and early insect development. Typical examples of Turing systems were introduced by Gierer and Meinhardt [15], Schnackenberg [45] and Thomas [47]. However, Turing Theory is still highly controversial for actual reaction-diffusion morphogen prepatterns in vivo. A major obstacle to its acceptance is the identification of the morphogens in early embryonic development. The fact that certain chemicals are essential for development does not necessarily mean that they are morphogens. So, Turing Theory may not be applicable to morphogenesis yet. The present work uses Turing mechanism to understand and predict about a certain type of cells called N2a cells in vitro. Roughly speaking, we want to study the effects of adding certain chemicals to a dish of cells. This is quite a distinct scenario from pattern formation in the early embryo stage.

The Turing mechanism has been successfully applied to some real biological pattern formation problems such as sea urchin shell patterns [3], patterns of the skin

of fish [7] and juxtacrine patterning with lateral inhibition [50]. Turing's work has been extended in many aspects for over a decade [4]. Formation of three dimensional patterns has been investigated in a number of reaction-diffusion systems (for example [8] and [24]). Schenk et al. proposed a three-component reaction-diffusion system capable of supporting interacting pulses in two spatial dimensions [44]. Most of the models exhibiting Turing pattern formation consist of a two component reaction-diffusion system, while in reality the signaling molecules corresponding to these two components also play important roles in cell differentiation and pattern formation that cannot be overlooked.

This is a recent interesting approach to Turing mechanism wherein activator and inhibitor are included into the biochemical context. In fact, for the first time, a network of signaling pathways is added to the Turing mechanism. The model proposed by E.M. Rauch and M.M. Millonas [38] makes use of signal transduction kinetics such that activator and inhibitor are transformed into the corresponding signaling molecules through a series of biological reactions. The present work utilizes the same approach for the production of a broken spatial symmetry. I develop a model analogous to their devised model to investigate the effects of Retinoic Acid (RA) and activated Notch on axon formation and neuronal differentiation. These are discussed in more detail in the next section where I will address the objectives and main purpose of this study.

1.4 External signals, symmetry breaking instabilities and Turing Theory

The nervous system is developed as a result of an orchestrated series of cell division, cell fate commitment and differentiation that give rise to specific cell types called neurons and glia. Each of these cell types demonstrates a specific structure. In particular, a neuron consists of a single axon (signal transmitter), a nucleus and a host of dendrites (Fig. 1.4 (a)). A key question in Mathematical Biology is how the fate of an axon is determined. It has been suggested that all processes have an equal potential to become an axon prior to neuronal differentiation [12]. But only one of the processes becomes committed to an axonal fate (Fig. 1.4 (b)). In a proposed molecular model of axon formation [1], it has been suggested that the regulation between the positive and negative feedback loops provides a robust mechanism for spontaneous symmetry breaking and formation of only one axon. The assumption is that positive and negative feedback factors form an intricate balance. When a feedback gets stronger, this balance will become unstable and eventually the symmetry between the neurites (processes) breaks and one of them starts growing faster than the other neurites. The one with the greatest rate of growth becomes an axon while the other neurites turn into dendrites and thus the cell differentiates to a neuron.

Positive and negative feedback loops appear in certain pathways of chemicals which are called signaling pathways. A signaling pathway includes a series of biological reactions that affect cell functions by targeting specific genes. In the present work there are two signaling pathways that I am concerned with: the Delta-Notch signaling pathway with a negative feedback loop and the Retinoic Acid (RA) pathway with a positive feedback. There are certain chemicals and proteins that may be utilized in an experiment, which we will refer to as external signals. External

signals play a crucial role in neuronal differentiation and axon formation. In fact, the strength of positive and negative feedback could be affected by certain external signals and consequently the symmetry between the neurites may be destabilized or become more stable. In our case Notch signals can antagonize neurite outgrowth in neuroblastoma cells [14] whereas experiments demonstrate that Retinoic Acid (RA) promotes neurite outgrowth in neuroblastoma cells. This suggests that Notch signals utilized in the experiment may have a positive effect on the balance between the positive and negative feedback while RA signals may destabilize this balance. In this study, Retinoic Acid with different concentrations and Notch1 (i.e. Notch1 intracellular domain, NICD) are two external signals which are utilized for N2a cells in vitro.

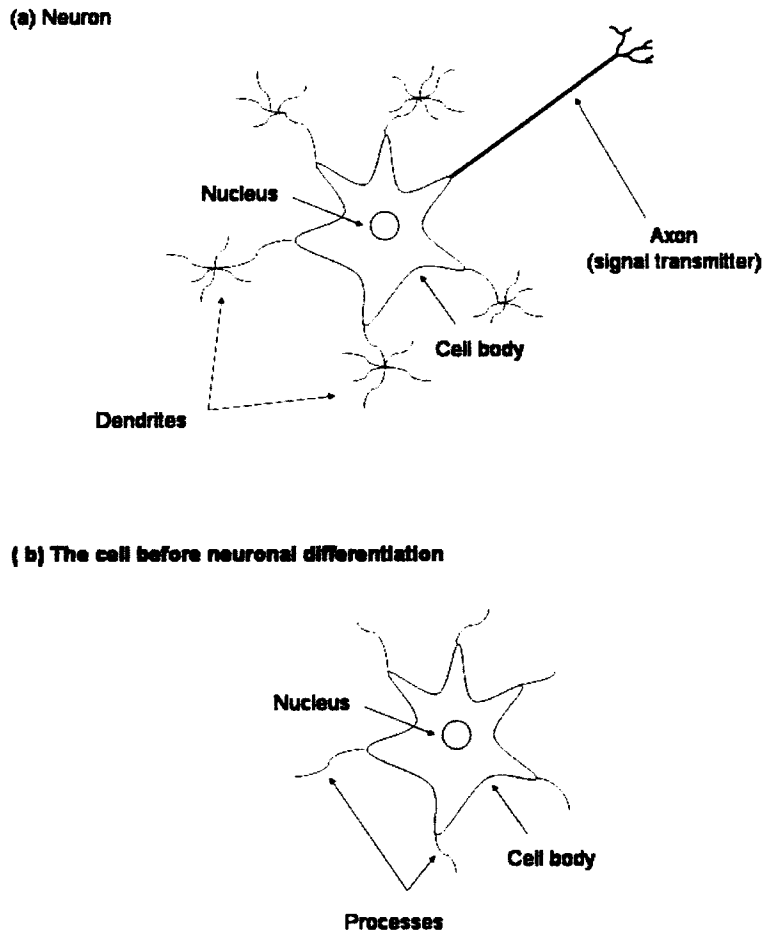

Figure 1.4 *(a) Neuron: A type of cell consisting of a single axon (signal transmitter), a nucleus and a host of dendrites. (b) Cell before differentiation: All neuronal processes have the potential to become an axon, but only one of the processes becomes committed to an axonal fate. Why?*

The purpose of this study is to answer the following questions:

1. What are the effects of external signals (RA and Notch1) on the symmetry breaking instabilities for axon formation?

2. Assuming an interaction between Delta-Notch and RA pathways, what would be the effects of this interaction on the whole system?

3. Is Turing Theory applicable to the problem of spontaneous symmetry breaking?

In Chapter 2, a mathematical model analogous to a devised model of biological pattern formation is proposed [38] to investigate the effect of external signals in the symmetry breaking instabilities for axon formation. The possible interaction between signaling pathways is considered as a perturbation to the system. In Chapter 3, linear stability analysis is used to derive the conditions for the existence of Turing instabilities for cases where the system is either perturbed or unperturbed. In Chapter 4, perturbation techniques are utilized to investigate the effects of perturbations on the stability of steady states and the symmetry breaking instabilities.It is also shown that under some conditions, small perturbations to the system do not change the qualitative behavior of the system. On the basis of the numerical results, a bifurcation analysis is provided in Chapter 5 in which Turing bifurcations and Hopf bifurcations are examined.

The outcomes of laboratory experimentations along with conclusions are presented in Chapter 6, where the applicability of the Turing mechanism to one of the problems in neurobiology as characterized above is discussed.

Chapter 2

The Mathematical Model

2.1 Introduction to the model

Lateral inhibition is a type of cell-cell interaction whereby a cell that adopts a particular fate inhibits adjacent cells from acquiring the same fate. It is known that Delta-Notch signaling is involved in the regulation of neural development through lateral inhibition. In fact, small differences in levels of Delta-Notch signaling between the cells in the proneural cluster allow one cell to advance farther along the pathway to neural specification than the others; it then sends signals that prevent the less advanced cells from adopting a neural fate. Lateral inhibition is affected by a negative feedback loop: the more inhibition a cell delivers to its neighbors, the less it receives back from them and the more it is consequently able to deliver [49]. The mechanism of lateral inhibition with feedback has been used in modeling Delta-Notch signaling for biological pattern formation and cell fate determination [9]. Collier and his colleagues showed that an initial slight difference of the level of Delta and activated Notch between neighbors will become self-amplifying, generating a full-blown spatial pattern of inhomogeneity. The significant outcome from

their work was the finding that lateral inhibition takes place only if the negative feedback is sufficiently strong. However, it remains unclear how the negative feedback may get sufficiently strong. This can be clarified if both positive and negative feedback are considered in the model of pattern formation. The regulation between the positive and negative feedback with the external signals may result in one of the feedbacks getting stronger than the others.

In our case, there is evidence that N2a neuroblastoma cells with high levels of Delta activity and low levels of Notch activation become neurons while cells with low Delta activity and high Notch activation levels remain undifferentiated [14]. Also, several experiments demonstrate that RA promotes neuronal differentiation in N2a cells. These suggest that the mechanism of lateral inhibition with both positive and negative feedback can be used to model the regulation of neurite outgrowth in N2a neuroblastoma cells.

The biochemical pathway of RA has been well studied in different types of cells. The chemicals produced from the metabolism of RA play an important role in the process of cell differentiation. The RA biochemical pathway has a direct effect on neurite outgrowth in neuroblastoma cells. This suggests that the RA biochemical pathway appears in a positive feedback: the higher concentration of RA is introduced to a cell, the greater potential each neurite has to grow further and become an axon. The Delta-Notch negative feedback must be generated simultaneously to assure the formation of only one axon. The process of neurite outgrowth and axon formation is equivalently considered as the process of neuronal differentiation, which is the result of the regulation between positive and negative feedback. As mentioned in Chapter 1, it can be hypothesized that positive and negative feedback form an intricate balance. As a feedback gets stronger, the balance may become unstable, which results in spontaneous symmetry breaking and eventual neuronal differentia-

tion. An important distinction between the positive and negative feedback is that the positive feedback exists only when RA is added to the system, while the negative feedback already exists in the system. Therefore, in the absence of RA external signals, there is no positive feedback to provide a potential for axon formation. And in this case, no axon formation is expected. Also, it is important to know that there is a threshold for the negative feedback. This means that the negative feedback must be sufficiently strong to support the mechanism of lateral inhibition [9], otherwise no axon formation is expected.

But how is it that a feedback may get stronger or weaker? I suggest that external signals, added to the system, diffuse into the cells and may strengthen or weaken the feedback. Here, it is hypothesized that activated Notch1 (i.e. Notch1 intracellular domain, NICD) utilized in the experiment weakens the negative feedback and RA added to the cells in vitro strengthens the positive feedback. Indeed, Notch signals antagonize neurite outgrowth and neuronal differentiation [14], which may be interpreted as a failure of the mechanism of lateral inhibition with negative feedback. Also, experiments show that higher concentrations of RA added to the N2a cells in vitro promotes neurite outgrowth which suggests that the positive feedback gets stronger with RA external signals. Absence of Notch signals corresponds to the case in which the negative feedback is sufficiently strong. In the absence of Notch signals adding a high concentration of RA signals to the system is expected to produce a positive feedback stronger than the negative feedback such that the symmetry between the neurites breaks and one of the neurits becomes an axon. Diffusion of the external signals (Notch and RA) into cells is crucial for production of a broken symmetry in cells differentiating to neurons. In the context of Turing Theory, perturbation by introduction of diffusion results in spatial pattern formation and cell differentiation.

There are a growing number of articles suggesting the relevance of the Turing mechanism to spontaneous symmetry breaking (see [43] for example). Here, the assumption is that there is a direct relation between the strength of the feedback loops and the diffusion of the signaling molecules, so that the perturbations by diffusion can be interpreted as the perturbations of feedback loops and vice-versa. The present work implements the Turing mechanism for the breaking of spatial symmetry in an initially homogeneous system of reacting and diffusing substances.

The concept of interacting signaling pathways can be used in mathematical models of biological pattern formation and cell differentiation [10]. Here, we may assume that Notch1 intracellular domain (NICD) slows down RA signals by blocking Retinoic Acid receptor (RAR) in the nucleus and that in a set of reactions RA catalyzes the production of Notch. This interaction is considered as a perturbation to the system. An aim of the present work is to establish and compare the conditions for spontaneous symmetry breaking for both cases where the system is either perturbed or unperturbed. In the next section the mathematical model is presented along with the main assumptions and the general kinetic schematic of the model.

2.2 Mathematical model of signaling pathways affected by external signals

It is often useful and intuitively helpful in model building to express the mechanism's kinetics in schematic terms with some convention to indicate positive and negative feedback loops, activation, inhibition and diffusion. Figure 2.2(a) is a diagrammatic representation of the effective negative feedback loop between Notch and Delta.

In neighboring cells, initially all cells can equally express Delta and Notch, but a change causes one cell to increase its expression of Delta. This leads the cell to deliver more inhibition to its neighbors (i.e. the production of Notch in neighboring cells increases) and receive less inhibition in return from them. The reception of less inhibition increases the production of more Delta in the cell and enables the cell to deliver more inhibition. In the end, the cell with a high level of Delta and a low level of Notch activity turns into a neuron while it has inhibited the neighboring cells from adopting a neuronal fate (i.e. the neighboring cells with a high level of Notch activity remain undifferentiated). The thickness of arrows in Figure 2.2 represents the strength of the feedbacks. Adding Notch external signals and a higher concentration of RA weakens the negative feedback and strengthens the positive feedback respectively (Figure 2.2(b)) such that the balance between the positive and negative feedback may break and result in axon formation.

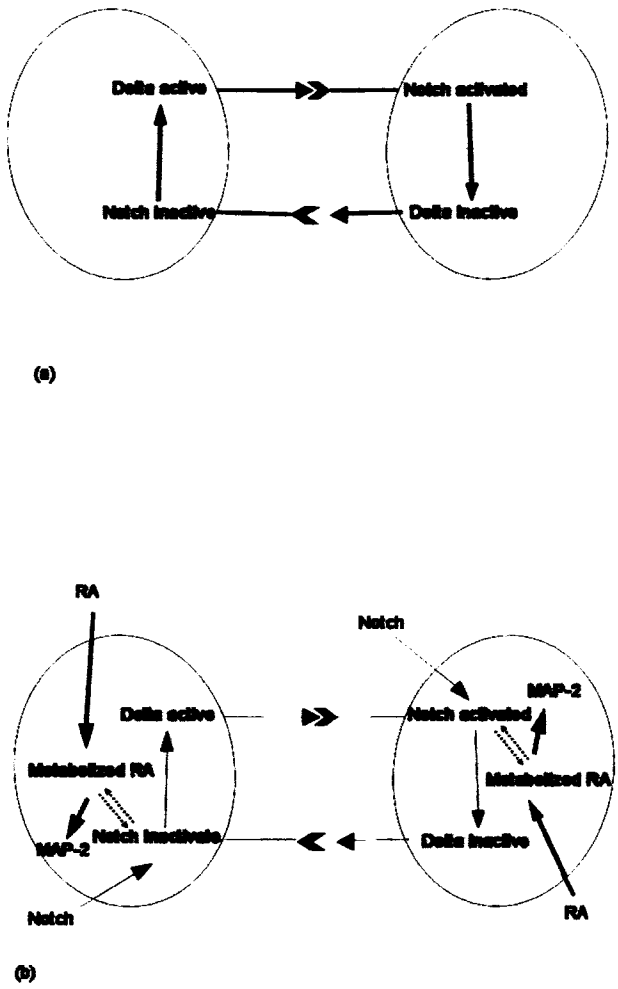

Figure 2.2 *(a) The effective negative feedback loop between Notch and Delta in two neighboring cells. [9] (see the text for more details).*

(b) The thickness of arrows represents the strength of the feedbacks such that, adding Notch external signals and a higher concentration of RA weakens the negative feedback and strengthens the positive feedback respectively. Possible interaction between Delta-Notch and RA signaling pathways is shown with dashed arrows.

In Figure 2.2(b) the general concept of adding external signals to the Delta-Notch system is schematized. External signals (RA and Notch) can directly diffuse into cells across the cell membranes. There does not exist any other transport of molecules across cell membranes. Instead, upregulation of Delta in a cell and upregulation of Notch in its neighbor may take place through the process of lateral inhibition. Also, upregulation of MAP-2 in each cell may happen through the biochemical pathway of RA. These are considered as diffusion of the signaling molecules inside the cells. Possible interaction between Delta-Notch and RA signaling pathways is shown with dashed arrows in Figure 2.2 (b) where RA signals may increase the rate of production of Notch and Notch signals may slow down RA signals in the process of metabolization of RA.

The present model extends that proposed by Rauch and Millonas [38] in two important respects. First, it takes into account the essential role of nonlinearity in the equations representing the transformation of activator and inhibitor into corresponding signaling molecules and the reverse transformation of the molecules into activator and inhibitor. Secondly, it is well known that lateral inhibition plays a key role in pattern formation and cell fate determination (see [25],[9] and [34]). The influential mechanism of lateral inhibition is a crucial factor in a system of feedback loops that is considered in the present model.

There are five assumptions to the model. The first three assumptions can be found in different models of biological pattern formation ([14],[9] and [1]), but the last two assumptions are specifically made for the present model:

1. Cells interact through feedback loops only with their adjacent cells.

2. The level of activated Notch and the concentration of RA in a cell determine cell differentiation: low levels of Notch and high concentrations of RA lead to

neuronal differentiation, otherwise a cell remains undifferentiated.

3. The symmetry between the neurites breaks only when a feedback gets stronger and the balance between the feedbacks becomes unstable.

4. The strength of feedback loops can be affected by external signals: activated Notch weakens the negative feedback and RA signals strengthen the positive feedback.

5. The system is perturbed by interactions between Notch and RA signaling pathways: NICD slows down RA signals by blocking Retinoic Acid receptor (RAR) in the nucleus and in a set of reactions RA catalyzes the production of more inhibitor (Notch).

The elements of the model are activated Notch protein (I), the level of Delta activity (M_I), concentration of RA in each cell (A) and the level of microtubule associated protein 2 (MAP-2) activity (M_A) in terms of local polymerization in each cell. (I) is the inhibitor with its messenger molecules M_I and (A) is the activator with its messenger molecules M_A. RA as an external signal with a positive feedback, catalyzes the production of MAP-2. The Notch-RA interaction is considered as a perturbation to the system.

Equations (2.2.1)-(2.2.4) represent the mathematical model proposed in this study to investigate the effects of external signals on axon formation and neuronal differentiation:

$$\frac{\partial A}{\partial t} = F_\alpha(A) + \epsilon S(A, \frac{I}{I_o}) + d_1 \nabla^2 A, \tag{2.2.1}$$

$$\frac{\partial \frac{I}{I_o}}{\partial t} = G_\alpha(\frac{I}{I_o}) + Y(\frac{M_I}{M_o}) + \epsilon \overline{S}(A, \frac{I}{I_o}) + d_2 \nabla^2 \frac{I}{I_o}, \tag{2.2.2}$$

$$\frac{\partial \frac{M_I}{M_o}}{\partial t} = -a_3 \frac{M_I}{M_o} + Z(\frac{I}{I_o}) + d_3 \nabla^2 \frac{M_I}{M_o}, \tag{2.2.3}$$

$$\frac{\partial M_A}{\partial t} = b_2 A - b_3 M_A + d_4 \nabla^2 M_A, \tag{2.2.4}$$

with initial conditions at $t = 0$:

$$A = M_A = 0, \tag{2.2.5}$$

$$I = I_o + h_I(r), \tag{2.2.6}$$

$$M_I = M_o + h_M(r), \tag{2.2.7}$$

where h_I and h_M are given functions and all the constants $b_2, b_3, a_3,...$ are positive. Diffusive transport of external signals and also transport of proteins between the segments of the same cell are included in the system. Coefficients d_1, d_2, d_3 and d_4 are the rates of diffusion related to each component. The rates of removal for M_I and M_A are a_3 and b_3 respectively. b_2 is the rate of production of M_A in the processes of signal transduction, I_o and M_o are typical levels of Notch and Delta activity chosen such that the functions Y and Z are of order 1. $\epsilon > 0$ is a small parameter which represents the interactions between the external positive signal (RA) and the inhibitory signal (Notch).

The parametric functions F_α and G_α represent the kinetics of RA and Notch signals. The functions Y and Z represent the interactions between Notch and Delta transmembrane proteins (i.e. Notch as ligand and Delta as its receptor). The functions S and $\overline{S}$ show the possible interactions between the signaling pathways.

All these functions are real continuous functions that will be defined in the next section.

2.3 Nondimensionalization and function specification

The present model, as described in [5], consists of two reaction-diffusion subsystems, one of which is the RA-MAP-2 subsystem represented in equations (2.2.1) and (2.2.4). The other one is the Delta-Notch subsystem represented in equations (2.2.2) and (2.2.3). Each subsystem is compelled by external signals which are concentration of RA and the level of activated Notch used in the experiment. This can be embodied by the form of the parametric function G_α used in the model. The two subsystems may interact through the functions S and $\overline{S}$ when $\epsilon > 0$. As mentioned in the fifth assumption of the model, RA may catalyze the production of Notch and in turn Notch may slow down the effect of RA signals. These two can be reflected in the functions $\overline{S}$ and S respectively. RA is removed with rate c_1 and Notch is produced with rate l_2:

$$S(A, \frac{I}{I_o}) = -c_1 \frac{I}{I_o}, \tag{2.3.1}$$

$$\overline{S}(A, \frac{I}{I_o}) = l_2 A, \tag{2.3.2}$$

where $c_1, l_2 > 0$. However, this choice of S could be troublesome since it can violate $A \geq 0$, in which case there is no biological interpretation for the perturbed system. Therefore, in this study, we exclude the case that A becomes negative and concentrate on the steady states with $A \geq 0$.

Nondimensionalization or problem normalization is the first and arguably the

most important step in the analysis of a system of differential equations. It involves scaling variables by a typical reference value to leave nondimensional variables whose typical scale is $O(1)$. This allows the identification of the dominant terms in equations and their interaction in different regimes which gives insight into the structure of solutions and the dominant physical mechanisms at work.

In our case, let L be a length scale, τ be a temporal scale and set:

$x^* = \frac{x}{L}$, $T = \frac{t}{\tau}$,

$u = A$, $q = M_A$, $v = \frac{I}{I_o}$, $w = \frac{M_I}{M_o}$,

$\gamma_1 = c_1 L^2$, $f_\alpha(u) = c_1^{-1} F_\alpha(A)$, $s(u,v) = c_1^{-1} S(A, \frac{I}{I_o})$,

$\gamma_2 = L^2$, $g_\alpha(v) = l_2^{-1} G_\alpha(\frac{I}{I_o})$, $y(w) = l_2^{-1} Y(\frac{M_I}{M_o})$, $\bar{s}(u,v) = l_2^{-1} S(A, \frac{I}{I_o})$,

$\gamma_3 = L^2$, $z(v) = Z(I)$

$\gamma_4 = L^2 b_2$, $a_4 = \frac{b_3}{b_2}$,

assuming $\tau \approx L^2$, corresponding to the diffusive time scale, then the non-dimensionalized form of the model is as follows;

$$u_t = \gamma_1 \left(f_\alpha(u) + \epsilon s(u,v) \right) + d_1 \nabla^2 u, \tag{2.3.3}$$

$$v_t = \gamma_2 \left(g_\alpha(v) + y(w) + \epsilon \bar{s}(u,v) \right) + d_2 \nabla^2 v, \tag{2.3.4}$$

$$w_t = \gamma_3 \left(-a_3 w + z(v) \right) + d_3 \nabla^2 w, \tag{2.3.5}$$

$$q_t = \gamma_4 \left(u - a_4 q \right) + d_4 \nabla^2 q, \tag{2.3.6}$$

where all the constants $\gamma_1, \gamma_2, a_3, \ldots$ are positive and the initial conditions at $t = 0$ become

$$u = q = 0, \tag{2.3.7}$$

$$v(0, \vec{r}) = v_o, \tag{2.3.8}$$

$$w(0, \vec{r}) = w_o. \tag{2.3.9}$$

Functions y and z represent the nondimensionalized form of the kinetics of the Delta-Notch signaling in the negative feedback loop. The rate of production of Notch activity in each cell is governed by the function y, which is a continuous increasing function of the level of Delta activity in neighboring cells. The rate of production of Delta activity in each cell is related to the function z which is a continuous decreasing function of the level of activated Notch in the same cell. Here, we take y and z to be of the same form as they are proposed in previous articles (e.g. [9]). $y, z : [0, \infty) \to [0, \infty)$.

$$y(x) = \frac{x^k}{c_2 + x^k}, \tag{2.3.10}$$

$$z(x) = \frac{1}{1 + c_3 x^h}, \tag{2.3.11}$$

where $c_2, c_3 > 0$ and $k, h \geq 1$. The parameter values we use in all proceeding discussion are $k = h = 2$.

Functions f_α and g_α represent the kinetics of RA and Notch signals in the absence of feedback loops. It is known that RA induces neuronal differentiation in many types of cells (see [30] for example). Also recall that Notch signals can antagonize neurite outgrowth in neuroblastoma cells [14]. These are two important factors that are reflected in the modeling of our problem in the following sense. Despite the production of Delta and Notch in the N2a cell, RA is not produced in the cells. Here, in each experiment, RA is constantly added to the system such that a constant inflow rate of RA is provided. Let the inflow rate of RA be $\frac{1}{\alpha}$ and its rate of removal

be a_1; then we can take the function f_α in the following form:

$$f_\alpha(x) = \frac{1}{\alpha} - a_1 x, \tag{2.3.12}$$

where $\alpha \in (0,1)$ (i.e. the value of α is normalized betwen zero and one) and $a_1 > 0$.

We may add RA with a different concentration in each experiment. By the function f_α we get that in the absence of RA-Notch interaction ($\epsilon = 0$), the concentration of RA in each cell will be proportional to $\frac{1}{\alpha}$. Figure 2.3(a) shows the behavior of RA external signals in each cell for $a_1 = 1$ and different values of α. Let the level of activated Notch used in the experiment be proportional to the parameter α, then,

$$g_\alpha(x) = \frac{a_2}{(\alpha - 1)}(x - \alpha)^2, \tag{2.3.13}$$

where $a_2 > 0$ and $\alpha \in (0,1)$. The parametric function g_α can be regarded as the amount of Notch removed in a time equal to the mean life time of Notch activity. This amount is considered to be inversely related to the level of activated Notch utilized in the experiment. As one can see in Figure 2.3(b), in the absence of RA-Notch interaction and Delta-Notch negative feedback (i.e. $y(w) = 0$), the level of Notch activity drops dramatically when the level of activated Notch used in the experiment is low (e.g. $\alpha = 0.1$). The initial value of Notch is considered to be one. As mentioned before, there is a threshold for the negative feedback such that it should be sufficiently strong to support the mechanism of lateral inhibition [9], otherwise no axon formation is expected. Adding RA with a lower (higher) concentration and using a higher (lower) level of activated Notch in experiments are subject to an increase (decrease) in the value of α in our model.

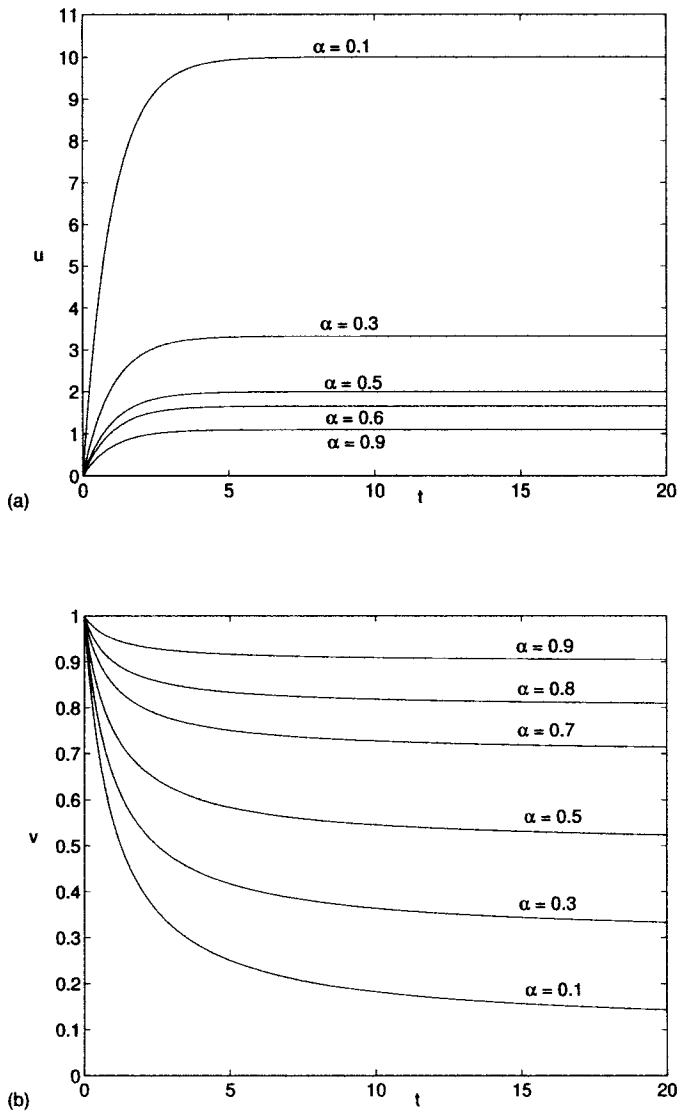

Figure 2.3 *(a) The behavior of RA external signals in each cell for* $a_1 = 1$ *and different values of* α. *(b) The effect of Notch external signals on Notch activity in each cell: in the absence of RA-Notch interaction and Delta-Notch negative feedback, the level of Notch activity drops dramatically when the level of activated Notch used in the experiment is low (e.g.* $\alpha = 0.1$*).*

In fact $f_\alpha \to \infty$ as $\alpha \to 0$ shows that the positive feedback function gets ultimately strong and $g_\alpha \to -\infty$ as $\alpha \to 1$ shows that the negative feedback function gets ultimately weak.

2.4 Solutions to reaction-diffusion equations

As the general form of reaction-diffusion equations was introduced in the first chapter, one may possibly think of solutions of reaction-diffusion equations with some initial or boundary conditions. This section is a short review of particular or general solutions to reaction-diffusion equations with a focus on the possible solutions of the present system of equations. There are many works investigating the existence of solutions of two-component reaction-diffusion equations ([20],[33],[41],[42]). For instance, different types of solutions were established for model systems of prey-predator interaction with diffusion and Gierer-Meinhardt equations for pattern formation of spatial tissue structures of morphogenesis [15]. There are large amplitude stationary solutions of Gierer-Meinhardt systems with zero flux boundary conditions ([26],[31]). Also, the existence of positive solutions to Gierer-Meinhardt systems with zero Drichlet boundary conditions was established by E. H. Kim ([22],[21]). Singular perturbation methods can be used to construct large amplitude solutions to boundary value problems of prey-predator systems with diffusion [27], where the stability of this type of solutions was studied a few years later [32].

Under some assumptions, certain types of solutions can be established for general systems of reaction-diffusion, i.e.

$$\frac{\partial \vec{c}}{\partial t} = f(\vec{c}) + D\nabla^2 \vec{c}, \tag{2.4.1}$$

where D is a diagonal matrix of positive diffusion constants and f is a vector field representing reaction kinetics. Let $f \in C^\infty$ and $f(\vec{0}) = \vec{0}$. In the absence of diffusion, the kinetic equations $\frac{\partial \vec{c}}{\partial t} = f(\vec{c})$ can be linearized at 0 to obtain $\frac{\partial \vec{c}}{\partial t} = A\,\vec{c}$. If the matrix of linearization A has a conjugate pair $p \pm iq$ of eigenvalues with $p > 0$ and the other possible eigenvalues of A lie in the left half of the complex plane (so that 0 is an unstable fixed point), then the general reaction-diffusion equation has a one-parameter family of plane wave solutions [23], i.e. solutions of the form

$$\vec{c}\,(\vec{z},t) = \vec{y}\,(\sigma t - \vec{k}\cdot\vec{z}), \tag{2.4.2}$$

where $\vec{y}$ is a 2π-periodic vector function of its argument, $\sigma > 0$ is the angular frequency and $\vec{k}$ is the wave number vector of the plane wave which propagates in the direction of $\vec{k}$ with speed $\sigma/\left|\vec{k}\right|$.

This has been proved and generalized to the case that the kinetic equations, $\vec{c}_t = f(\vec{c})$, instead of an unstable fixed point, have a limit cycle [23]. Our model has been formulated as a system of four reaction-diffusion equations; hence, the work by N. Kopell and L. N. Howard [23] can be applied to show the existence of plane wave solutions for the present model system. Furthermore, let the system have a limit cycle or an unstable fixed point with related eigenvalues in the form mentioned before, then the system admits a one-parameter family of plane-wave solutions, and near the fixed point or the limit cycle, these solutions can be parametrized by $\left|\vec{k}\right|^2$. Also, the solutions tend to the limit-cycle solution of $\vec{c}_t = f(\vec{c})$ or the fixed point related to the linearized form of the kinetic equations (i.e. $\vec{c}_t = A\,\vec{c}$).

These types of solutions are called "slowly varying waves". They are vector-valued functions which locally resemble a plane wave, but which have local wave number and local frequency that vary on a large scale. Spatially, "large" means

many wavelengths; temporally, it means many periods [19]. It is not difficult to find the conditions for the present system to have this type of solution, but another type of solutions is the interest of the present work.

The following theorem can be used to show the existence of solutions for the present model system with zero Drichlet or Neumann boundary condition (i.e. zero flux boundary condition).

Theorem: Let $\frac{\partial \vec{c}}{\partial t} = f(\vec{c}) + D\nabla^2 \vec{c}$ be a system of reaction-diffusion equations with given initial condition $\vec{c}\ (0, \vec{r}) = \vec{c}_o, \vec{r} \in \mathbb{R}^L$, where D is the diagonal $L \times L$ matrix of positive diffusion constants $f \in H^{K,P}(M, \mathbb{R}^L)$, and $K > 2 + n/p$ such that $H^{K,P}(\cdot, \cdot)$ is L^p-Sobolev space and $M \subset \mathbb{R}^n$ is closed and bounded. Suppose that

$$f(\vec{y}) \cdot \vec{N} < 0 \text{ for all } y \in \partial R, \tag{2.4.3}$$

where $R = \{y \in \mathbb{R}^L, a_j \leq y_j \leq b_j\}$ and $\vec{N}$ is the outer normal to R. If f take values in the interior $\dot{R}$ of R, then the solution to the system exists and takes values in interior $\dot{R}$ for all $t > 0$.

The proof of this theorem can be found in advanced books on partial differential equations and it can be generalized to zero Drichlet or zero flux boundary condition (see for example [46]). For the present model, one can simply choose the parameter α and the constants such that the conditions for existence of solutions are satisfied. But the fact that f must take values in the interior of R is too restrictive for analysis of pattern formation and neuronal differentiation. To study the symmetry breaking instabilities for axon formation, the usual eigenfunction method is used in the next chapter to construct solutions for the present system linearized about the steady state $\vec{c} = 0$, subject to given initial conditions and zero flux boundary conditions.

The next chapter follows with the linear stability analysis of the system where the conditions for the existence of Turing instabilities are derived and compared for both cases where the two subsystems are either perturbed or unperturbed.

Chapter 3

Analysis of Axon Formation

3.1 Linear stability analysis of the system

In this section, study of the axon-forming potential of the present model begins by analyzing the stability of the homogeneous steady states. The analysis of axon formation presented in this section and the next have been published earlier this year [6]. By substituting the specified form of the functions in the present model, the dimensionless system of partial differential equations takes the form:

$$u_t = \gamma_1 \left(\frac{1}{\alpha} - a_1 u - \epsilon v \right) + d_1 \nabla^2 u, \tag{3.1.1}$$

$$v_t = \gamma_2 \left(\frac{a_2}{(\alpha - 1)} (v - \alpha)^2 + \frac{w^2}{c_2 + w^2} + \epsilon u \right) + d_2 \nabla^2 v, \tag{3.1.2}$$

$$w_t = \gamma_3 \left(-a_3 w + \frac{1}{1 + c_3 v^2} \right) + d_3 \nabla^2 w, \tag{3.1.3}$$

$$q_t = \gamma_4 \left(u - a_4 q \right) + d_4 \nabla^2 q. \tag{3.1.4}$$

For the present model, it is important to show that there exists at least one homogeneous steady state for which a linear stability analysis can be presented. By setting the coefficients of our system of equations (3.1.1)-(3.1.4) to: $a_1 = a_2 = 1$, $a_3 = 0.2$, $a_4 = 1$, $c_2 = 10\alpha$, $c_3 = 100\alpha$, $\gamma_1 = \gamma_2 = \gamma_4 = 1$ and $\gamma_3 = 50$, numerical results reveal that for $\alpha \in (0, 1)$ the system admits up to four steady states. For example, $\alpha = 0.5$ and $\epsilon = 0.02$ result in the homogeneous steady states $(u, v, w, q) =$ $(1.9872, 0.6418, 0.0600, 1.9872)$, $(1.9931, 0.3455, 0.2010, 1.9931)$, $(1.9976, 0.1201,$ $1.2864, 1.9976)$ and $(2.0013, -0.0646, 2.7247, 2.0013)$. The last steady state has a negative value for v, for which there is no physical or biological interpretation. The present work is concerned with steady states with all components greater than or equal to zero.

As mentioned in the previous chapter, the possible interaction between RA and Notch signaling pathways is considered as a perturbation to the system. The main purpose of this section is to derive the necessary and sufficient conditions for axon formation for the case where the two subsystems are unperturbed (i.e. $\epsilon = 0$). The next chapter continues with deriving the conditions for the case that the system is perturbed (i.e. $\epsilon > 0$). In the following the subscript ϵ indicates the case in which perturbation is considered (i.e. $\epsilon > 0$) and the subscript 0 indicates the case in which the system is not perturbed (i.e. $\epsilon = 0$).

In the case that the system is unperturbed, it is important to introduce a certain type of steady state that represents reduction of the system to a Delta-Notch subsystem. In the absence of an RA signaling pathway, the positive feedback is not generated to provide a potential for neurites to become an axon. In fact, it is known that in the absence of RA signals in each N2a cell, there is enough Notch to inhibit neuronal differentiation and axon formation. So in the case that no RA is used in the experiment, no axon formation is expected. Absence of an RA signaling

pathway will reduce the general system to the Delta-Notch subsystem (i.e. only equations (3.1.2) and (3.1.3) are considered here). In this case, the concentration of RA and MAP-2 are considered to be zero for all time (i.e. $u_o = q_o = 0$) and $(0, v_o, w_o, 0)$ represents the related homogeneous steady state. We call $(0, v_o, w_o, 0)$ an axon-free steady state where there is no axon formation expected and cells may remain undifferentiated.

Let $(u_\epsilon, v_\epsilon, w_\epsilon, q_\epsilon)$ be a homogeneous steady state of our general system; by linearizing the dimensionless model presented in equations (2.3.3)-(2.3.6) about the steady state, we get that

$$\frac{d\,\vec{R}_\epsilon}{dt} = A_\epsilon\,\vec{R}_\epsilon, \tag{3.1.5}$$

$$A_\epsilon = \begin{pmatrix} \gamma_1 f_u & -\epsilon\gamma_1 & 0 & 0 \\ \epsilon\gamma_2 & \gamma_2 g_v & \gamma_2 y_w & 0 \\ 0 & \gamma_3 z_v & -\gamma_3 a_3 & 0 \\ \gamma_4 & 0 & 0 & -a_4\gamma_4 \end{pmatrix}, \vec{R}_\epsilon = \begin{pmatrix} u - u_\epsilon \\ v - v_\epsilon \\ w - w_\epsilon \\ q - q_\epsilon \end{pmatrix}, \tag{3.1.6}$$

where $\left|\vec{R}_\epsilon\right|$ is small enough and A_ϵ is the coefficient matrix associated with the linearized system near the steady state $(u_\epsilon, v_\epsilon, w_\epsilon, q_\epsilon)$. The eigenvalues (λ_ϵ) are found for the solutions in the form:

$$\left\|\vec{R}_\epsilon\right\| \propto e^{\lambda_\epsilon t}, \tag{3.1.7}$$

where λ_ϵ is the eigenvalue perturbed by interactions between RA and Notch signaling pathways and $\|\cdot\|$ denotes the Euclidean norm.

Turing (diffusion-driven) instability occurs when in the absence of any spatial

variation, the homogeneous steady state is stable and it is unstable to spatial variations. In the following, the necessary and sufficient conditions for Turing instability of the steady states for the case $\epsilon = 0$ are derived. By letting $\epsilon \to 0$, we have $A_\epsilon \to A_o$ and $\lambda \to \lambda_o$ which implies $|A_o - \lambda_o I| = 0$. So, the eigenvalues of A_o are the roots of the following polynomial of λ_o:

$$(\lambda_o + a_4\gamma_4)(\lambda_o - \gamma_1 f_{u_o})(\lambda_o^2 + (\gamma_3 a_3 - \gamma_2 g_{v_o})\lambda_o - \gamma_2\gamma_3(a_3 g_{v_o} + y_{w_o} z_{v_o})) = 0. \quad (3.1.8)$$

Hence, the unperturbed eigenvalues are $\lambda_o^{(1)} = -a_4\gamma_4$, $\lambda_o^{(2)} = \gamma_1 f_{u_o} = -\gamma_1 a_1$, which are always negative (since, $a_1, a_4, \gamma_1, \gamma_4 > 0$), and

$$\lambda_o^{(3)}, \lambda_o^{(4)} = \frac{1}{2}\left\{(\gamma_2 g_{v_o} - \gamma_3 a_3) \pm \sqrt{(\gamma_2 g_{v_o} - \gamma_3 a_3)^2 + 4\gamma_2\gamma_3(a_3 g_{v_o} + y_{w_o} z_{v_o})}\right\}. \quad (3.1.9)$$

The homogeneous steady state $\vec{R_o}=\vec{0}$ is linearly stable if $Re(\lambda_o) < 0$ for any eigenvalue of A_ϵ. For the case $\epsilon = 0$, it is not hard to find the related conditions for linear stability. Here, in order to have $Re(\lambda_o^{(3)})$ and $Re(\lambda_o^{(4)}) < 0$, the following conditions are required:

$$P_o \equiv \gamma_2 g_{v_o} - a_3\gamma_3 < 0, \quad (3.1.10)$$

$$Q_o \equiv a_3 g_{v_o} + y_{w_o} z_{v_o} < 0. \quad (3.1.11)$$

These conditions are necessary for Turing instability of the steady state and initiation of symmetry breaking for axon formation. To find the sufficient conditions for Turing instability, the general dimensionless system (2.3.3)-(2.3.6) should be considered with initial and boundary conditions. In our case, it is physically reasonable to take zero flux boundary conditions. The initial boundary value problem is then

defined by:

$$\frac{\partial \vec{X}_\epsilon}{\partial t} = F(\vec{X}, \epsilon, \alpha) + D\nabla^2 \vec{X}_\epsilon, \tag{3.1.12}$$

$$(\vec{n} \cdot \nabla) \begin{pmatrix} u \\ v \\ w \\ q \end{pmatrix} = 0, r \text{ on } \partial B, \tag{3.1.13}$$

$$u(\vec{r}, 0) = q(\vec{r}, 0) = 0, \tag{3.1.14}$$

$$w(\vec{r}, 0) = v(\vec{r}, 0) = \text{given}, \tag{3.1.15}$$

where F is a parametric vector function with perturbation parameter ϵ and bifurcation parameter α, which represents the kinetic equations, ∂B is the closed boundary of the reaction diffusion domain B, $\vec{n}$ is the unit outward normal to ∂B and

$$D = \begin{pmatrix} d_1 & 0 & 0 & 0 \\ 0 & d_2 & 0 & 0 \\ 0 & 0 & d_3 & 0 \\ 0 & 0 & 0 & d_4 \end{pmatrix}. \tag{3.1.16}$$

For $\epsilon = 0$, the full reaction-diffusion system (3.1.12)-(3.1.15) linearized about the steady state $\vec{R}_o = \vec{0}$ is given by:

$$\frac{d \vec{R}_o}{dt} = A_o \vec{R}_o + D\nabla^2 R_o, \tag{3.1.17}$$

$$(\vec{n} \cdot \nabla)\, \vec{R_o} = 0, \text{ for } \vec{r} \text{ on } \partial B, \tag{3.1.18}$$

where

$$R_o(\vec{r}, 0) = \begin{pmatrix} u - u_o \\ v - v_o \\ w - w_o \\ q - q_o \end{pmatrix}. \tag{3.1.19}$$

In a usual way to solve the initial boundary value problems of this form, let

$$\vec{R_o}\,(\vec{r}, t) = \vec{W}\,(\vec{r}) \cdot T(t), \tag{3.1.20}$$

where $\vec{W}\,(\vec{r})$ is the time-independent solution of the spatial eigenvalue problem defined by

$$\nabla^2\, \vec{W} + k^2\, \vec{W} = 0, \tag{3.1.21}$$

$$(\vec{n} \cdot \nabla)\, \vec{W} = 0 \text{ for } \vec{r} \text{ on } \partial B, \tag{3.1.22}$$

where k is the eigenvalue. Here, the domain is considered to be one-dimensional; let $0 \leq x \leq L$ be the domain. Then the spatial eigenfunctions are $\cos(\frac{n\pi x}{L})$ and the solution of (3.1.21) and (3.1.22) is in the form

$$\vec{W}\,(x) = \sum_n \vec{a}_n \cos(\frac{n\pi x}{L}), \tag{3.1.23}$$

The solution satisfies the zero flux conditions at $x = 0$ and $x = L$. The eigenvalues in this case are $k = n\pi/L$, which is called the wave number and $1/k$ is proportional to the wavelength w; $w = 2\pi/k = 2L/n$ in our study. From now on, k is referred

to in this context. With bounded domains, there is a discrete set of possible wave numbers since n is an integer. Let $\vec{W}_k\ (x)$ be the eigenfunction corresponding to the wave number k. Each eigenfunction $\vec{W}_k$ satisfies zero flux boundary conditions. The function $T(t)$ can be specified by substituting (3.1.20) into (3.1.17). Using (3.1.21) implies that $T(t)$ has the exponential form of $e^{\lambda_o t}$, where λ_o is the eigenvalue which determines temporal growth. Because the problem is linear, the solution of boundary value problem (3.1.17)-(3.1.19) is in the form

$$\vec{X}_o\ (x,t) = \sum_{n=1}^{\infty} \vec{c}_n\ e^{\lambda_o t}\ \vec{W}_n\ (t) = \sum_{n=1}^{\infty} \vec{c}_n\ e^{\lambda_o t} \cos(kx), \tag{3.1.24}$$

where the constants $\vec{c}_n$ are determined by the Fourier expansion of the initial conditions in terms of $\vec{W}_n\ (r)$

Substituting this form into (3.1.17) with (3.1.21) implies, for each n,

$$\lambda_o\ \vec{W}_n = A_o\ \vec{W}_n + D\nabla^2\ \vec{W}_n = A_o\ \vec{W}_n - Dk^2\ \vec{W}_n\ . \tag{3.1.25}$$

The nontrivial solutions of $\vec{W}_n$ are determined by the roots of the characteristic polynomial

$$\left|\lambda_o I - A_o + Dk^2\right| = 0. \tag{3.1.26}$$

Evaluating the determinant with A_o and D from (3.1.16) and (3.1.6), the eigenvalues $\lambda_o(k)$ are functions of the wave number k. For the steady state to be unstable to spatial disturbances, at least one of the eigenvalues must have positive real part for some $k \neq 0$ (i.e. $Re(\lambda_o(k)) > 0$ for some $k \neq 0$). By solving (3.2.1), $\lambda_o^{(1)}(k) = -\gamma_4 a_4 - k^2 d_4$ and $\lambda_o^{(2)}(k) = -\gamma_1 a_1 - k^2 d_1$, since all the constants $\gamma_4, a_4, \ldots > 0$, then

$\lambda_o^{(1)}(k), \lambda_o^{(2)}(k) < 0$ for all $k \in \mathbb{R}$. $\lambda_o^{(3)}(k)$ and $\lambda_o^{(4)}(k)$ are the roots of

$$\lambda_o^2 + (k^2(d_2 + d_3) - P_o)\lambda_o + h(k) = 0, \tag{3.1.27}$$

where

$$h(k^2) = d_2 d_3 k^4 + (d_2\gamma_3 a_3 - d_3\gamma_2 g_{v_o})k^2 - \gamma_2\gamma_3 Q_o. \tag{3.1.28}$$

Similar to the work by Murray ([29],Chapter 2), the coefficient of λ_o is greater than zero since $d_2, d_3 > 0$ and by condition (3.1.10), $P_o < 0$. So, the only way to have one of the roots with positive real part is $h(k^2) < 0$ for some $k \neq 0$.
Since $Q_o < 0$ from (3.1.11), the only way for $h(k^2)$ to be negative is that $d_2\gamma_3 a_3 - d_3\gamma_2 g_{v_o} < 0$ and the minimum $h_{\min}(k) < 0$. For the case $\epsilon = 0$, these two conditions are equivalent to the following inequalities:

$$T_0 \equiv \gamma_2 g_{v_0} D_1 - \gamma_3 a_3 > 0, \tag{3.1.29}$$

$$-\gamma_2\gamma_3 Q_0 < \frac{T_0^2}{4D_1}, \tag{3.1.30}$$

where $D_1 = \frac{d_3}{d_2}$ is the diffusion ratio. One should note that if $h_{\min} > 0$, then all eigenvalues will take negative real parts which in the context of Turing Theory means that no axon formation is expected. So, for our system $h_{\min} = 0$ can define a bifurcation point. This is usually referred to as a Turing bifurcation and is studied in Chapter 5.

The conditions (3.1.10),(3.1.11),(3.1.29) and (3.1.30) are necessary and sufficient conditions for Turing instsbility of steady states for the case that the general system is unperturbed (i.e. $\epsilon = 0$). By solving $h(k^2) = 0$, one can find a range of unstable wave numbers of the system in which the steady state is linearly stable, but spatially

unstable. Within the unstable range, $Re(\lambda(k^2)) > 0$ has a maximum for the wave number k_m. This implies that there is a fastest growing mode in (3.1.24) for $\vec{X}_o$. Here, k_m^2 is the value that minimizes the function $h(k^2)$:

$$k_m^2 = T_o/2d_3. \tag{3.1.31}$$

By changing the parameter value of α, the unperturbed system may perform different ranges of unstable waves. Fig. 3.1 is the plot of the largest of the eigenvalues $\lambda(k^2)$ for several values of parameter α. The system admits Turing-type patterns when $0.3625 < \alpha < 0.58$. For each value of α in the interval (0.3625,0.58), there is a range of unstable wave numbers which is the interval on the k^2 axis with positive values of $Re(\lambda)$.

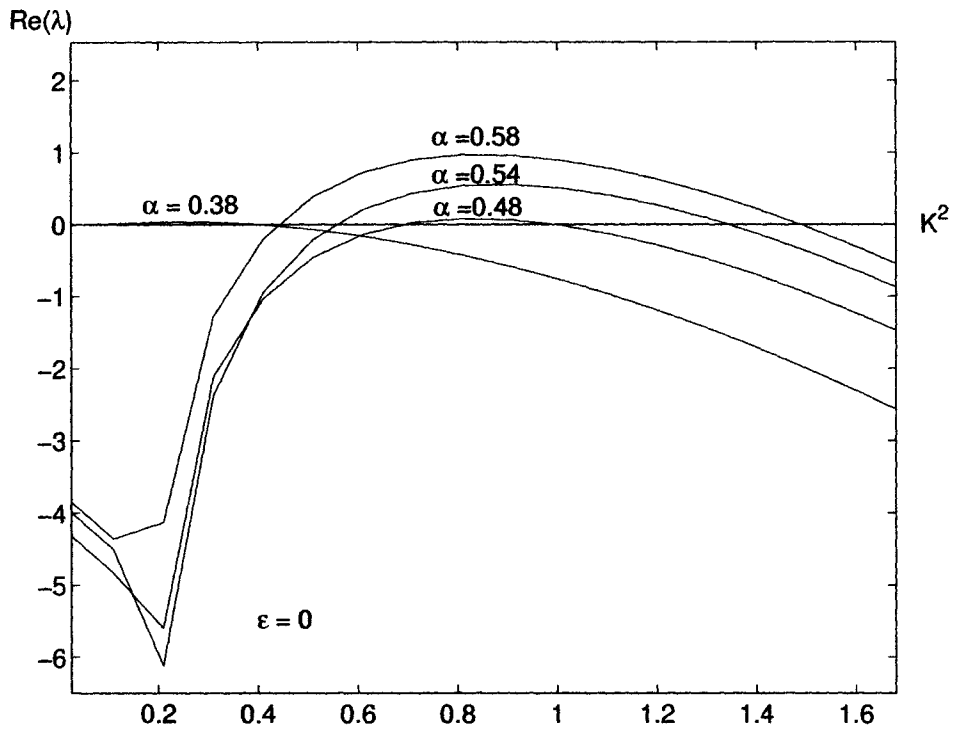

Figure 3.1 .Plot of the largest of the eigenvalues $\lambda(k^2)$. *The system admits Turing-type patterns when* $0.3625 < \alpha < 0.58$. k *corresponds to wave number.*

3.2 Axon formation in the presence of RA-Notch interaction

This section is focused on the case where both subsystems are perturbed (i.e. $\epsilon > 0$). As a continuation of the last section, first conditions for Turing instability are derived and then they are compared with the results of the last section. The eigenvalues of the linearized system for $\epsilon > 0$ are obtained by solving

$$\left|A_\epsilon - \lambda_\epsilon I - k^2 D\right| = 0, \tag{3.2.1}$$

where D is the diagonal matrix of diffusion coefficients and k corresponds to the wave number. One immediate eigenvalue of the linearized system is $\lambda = -a_4\gamma_4 - d_4k^2$ which is negative for all $k \in \mathbb{R}$; so the determinant (3.2.1) is reduced to a polynomial of degree 3 in the following form:

$$P_3(\lambda_\epsilon) = \lambda_\epsilon^3 + a_1\lambda_\epsilon^2 + a_2\lambda_\epsilon + a_3, \tag{3.2.2}$$

where:

$$a_1 = h_1 + h_2 + h_3, \tag{3.2.3}$$

$$a_2 = h_1h_2 + h_2h_3 + h_1h_3 + L_2 + L_1\epsilon^2, \tag{3.2.4}$$

$$a_3 = h_1h_2h_3 + L_2h_1 + L_1h_3\epsilon^2, \tag{3.2.5}$$

$$h_1 = d_1k^2 - \gamma_1 f_u, \tag{3.2.6}$$

$$h_2 = d_2k^2 - \gamma_2 g_v, \tag{3.2.7}$$

$$h_3 = d_3k^2 + a_3\gamma_3, \tag{3.2.8}$$

$$L_1 = -\gamma_1\gamma_2 s_v \bar{s}_u \text{ and} \tag{3.2.9}$$

$$L_2 = -\gamma_2\gamma_3 y_w z_v. \tag{3.2.10}$$

For $k = 0$, one can simply observe that

$$P_o \equiv -(h_2 + h_3) \text{ and} \tag{3.2.11}$$

$$Q_o \equiv \frac{-1}{\gamma_2\gamma_3}(h_2 h_3 + L_2). \tag{3.2.12}$$

Proposition 3.1

The following conditions (3.2.13) and (3.2.14) are sufficient for linear stability in the absence of spatial variations (i.e. $k = 0$).

$$P_\epsilon \equiv P_o - \frac{L_1}{h_1}\epsilon^2 < 0 \text{ and} \tag{3.2.13}$$

$$Q_o < 0. \tag{3.2.14}$$

Proof.

Given the properties of the functions in the system, L_1, L_2, h_1 and h_3 in equations (3.2.3)-(3.2.12) are always positive for all values of the parameters and coefficients. But h_2 can take positive or negative values. From conditions (3.2.13) and (3.2.14), one finds that $a_2 > 0$. Condition (3.2.13) is valid for all $\epsilon > 0$ which implies that $h_2 + h_3 \geq 0$. Since $h_1 > 0$, then $a_1 > 0$ and finally multiplying (3.2.14) by $-h_1$ and adding $L_1 h_3 \epsilon^2$ to it confirms that $a_3 > 0$. Hence, all coefficients of $P_3(\lambda)$ in (3.2.2) are positive. Since $P_3(\lambda)$ is of degree 3 with positive coefficients, it has one real

negative root. Rewrite $P_3(\lambda_\epsilon)$ in the following form:

$$P_3(\lambda_\epsilon) = (\lambda_\epsilon + r)(\lambda_\epsilon^2 + p\lambda_\epsilon + q), \tag{3.2.15}$$

where

$$p = a_1 - r, \tag{3.2.16}$$

$$q = a_2 - rp, \tag{3.2.17}$$

$$-r = \frac{b}{6} + \frac{1}{b}(2a_2 - \frac{2}{3}a_1^2) - \frac{a_1}{3} \text{ and} \tag{3.2.18}$$

$$b = 36a_1a_2 - 108a_3 - 8a_1^3 + 12(12a_2^3 - 3a_2^2a_1 - 54a_1a_2a_3 + 81a_3^2 + 12a_3a_1^3)^{\frac{1}{3}}. \tag{3.2.19}$$

The system is linearly stable if $Re(\lambda_\epsilon^{(i)}) < 0$ for $k = 0$ $(i = 1, 2, 3)$, where λ_ϵ^i's are the roots of the polynomial $P_3(\lambda_\epsilon)$. This is satisfied only if p and q are both positive. Condition (3.2.13) implies that $h_2 + h_3 \geq 0$, but $h_1 > 0$ and therefore,

$$a_1 \geq h_1. \tag{3.2.20}$$

Let $\epsilon > 0$ small enough such that

$$h_1 \geq \frac{L_1\epsilon^2}{h_1}. \tag{3.2.21}$$

Then,

$$a_2 \geq h_2h_3 + L_2 + \frac{h_3L_1}{h_1}\epsilon^2. \tag{3.2.22}$$

Note that with the given parameter values $h_1 \geq 1$ Condition (3.2.14) guarantees that the right hand side of (3.2.22) is positive; so by multiplying (3.2.20) and (3.2.22),

$$a_1a_2 > a_3. \tag{3.2.23}$$

Assume $p < 0$; then from $P_3(-r) = 0$ in (3.2.2), $r^2 p < 0$ is equivalent to $a_2 r - a_3 < 0$. Also, $a_2 p = a_1 a_2 - a_2 r < 0$. The last two inequalities imply that $a_1 a_2 < a_3$ which is in contradiction with (3.2.23). So, $p > 0$ for $k = 0$. $q = a_2 - rp = a_2 - r a_1 + r^2$ and therefore $rq = a_3$ with $r > 0$, but $a_3 > 0$, which implies that $q > 0$ for all $k \geq 0$. $\diamondsuit$

With properties of the functions in the system, L_1, L_2 and h_1 are always positive for all values of the parameters and coefficients. So, the conditions (3.2.13) and (3.2.14) are weaker than (3.1.10) and (3.1.11). This means that the steady states of the perturbed system are more likely to be linearly stable. The interaction between RA and Notch signaling pathways may have a positive effect on the linear stability of the homogeneous steady states of the system. However, it is too early to comment about the effects of this interaction on the symmetry breaking instabilities and the potential of axon formation in each cell. In the framework of Turing Theory, the analysis of axon formation is continued for the case that diffusion is present and the steady state is unstable to some spatial variations.

Proposition 3.2

Let $b : (0, \infty) \to \mathbb{R}$ be the real valued function of k defined in the form

$b = 36a_1a_2 - 108a_3 - 8a_1^3 + 12(12a_2^3 - 3a_2^2a_1 - 54a_1a_2a_3 + 81a_3^2 + 12a_3a_1^3)^{\frac{1}{3}}$,

and $\sigma : (0, \infty) \times (0, \infty) \to \mathbb{R}$ be the function of diffusion ratios in the form

$\sigma = -8(D_1 + D_2 + 1)(D_1^2 + D_2^2 + 1) + 20(D_1 + D_2 + 1)(D_1 + D_2 + D_1D_2) - 108D_1D_2$,

where $D_1 = \frac{d_3}{d_2}$ and $D_2 = \frac{d_1}{d_2}$ are the ratios of diffusion coefficients.

Suppose:

1. There exists a $k \in (0, \infty)$ with $k > k_T$ such that

$$b(k) \in (-\infty, 0) \setminus [x_1, x_2], \tag{3.2.24}$$

where k_T, x_1 and x_2 are known constants.

2. There exists $A \subset (0,\infty) \times (0,\infty)$, such that

$$\sigma(x,y) > 0, \tag{3.2.25}$$

for all $(x,y) \in A$.

Then the steady states of the perturbed system are unstable to spatial variations in a bounded range of unstable wave numbers (i.e. $[k_1, k_2]$) in the presence of interaction between RA and Notch signaling pathways.

Proof.

Since q is always positive, it follows from (3.2.13) that the only way to have $Re(\lambda_j) > 0$ for some $k > 0$ and $j = 1, 2$ is that $p < 0$. From (3.2.16) and (3.2.18),

$$p = \frac{b}{6} + \frac{T}{b} + B, \tag{3.2.26}$$

where $T = 2a_2 - \frac{2}{3}a_1^2$ and $B = \frac{2}{3}a_1 > 0$.

Consider $b \in (-\infty, 0)$ as a variable and assume that $T > 0$; then in the worst case senario there exists an interval $[x_1, x_2]$, such that (see Figure (3.2.a))

$$p < 0 \text{ for } b \in (-\infty, 0) \setminus [x_1, x_2]. \tag{3.2.27}$$

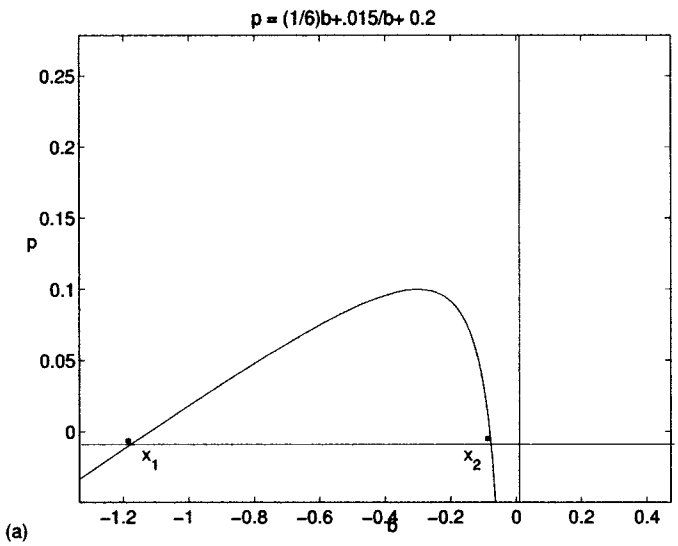

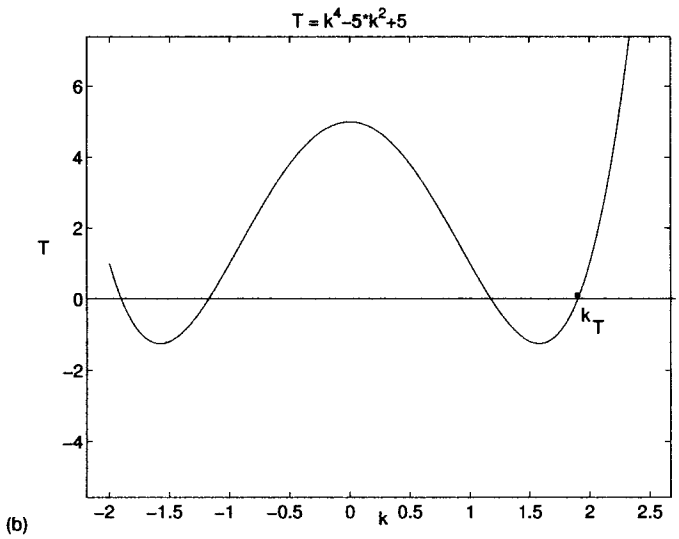

Figure 3.2 *(a) Consider $b \in (-\infty, 0)$ as a variable and assume that $T > 0$; then there exists an interval $[x_1, x_2]$, such that $p < 0$ for $b \in (-\infty, 0) \setminus [x_1, x_2]$. (b) By condition (3.2.25), it follows that $s_1 > 0$. Hence, there exists k_T such that $\forall k \geq k_T, T > 0$*

Considering equations (3.2.3)-(3.2.10), it follows that T is a polynomial of k of degree 4 in the following form:

$$T \equiv T_4(k) = s_1 k^4 + s_2 k^2 + s_3. \tag{3.2.28}$$

By condition (3.2.25), it follows that $s_1 > 0$. Hence, there exists k_T such that $\forall k \geq k_T, T > 0$ (see Figure (3.2.b)). Therefore, by equation (3.2.26), it follows that for each $k > k_T$, if $b < 0$, then there exists an interval $[x_1, x_2]$, such that $p < 0$ for b $\notin [x_1, x_2]$.

By condition (3.2.24) and continuity of b, there exists an interval $[k_1, k_2] \subset [k_T, \infty]$, such that $\forall k \in [k_1, k_2], b(k) \in (-\infty, 0) \setminus [x_1, x_2]$ and $T(k) > 0$. By equation (3.2.26), for $b = b(k)$ and $T = T(k) \forall k \in [k_1, k_2]$, p takes negative values. So, in the interval $[k_1, k_2], A_\epsilon$ has at least one eigenvalue with positive real part which means that the homogeneous steady state is spatially heterogeneous (unstable to the spatial variations). Since k corresponds to wave number, it is physically reasonable that spatial inhomogeneity occur only in bounded intervals of k. So, it is necessary to assure that p will not be negative after a certain value of k. By equations (3.2.3)-(3.2.10), it follows that b as a function of k has the form

$$b = \sigma_b k^6 + \text{Lower order terms}, \tag{3.2.29}$$

where

$\sigma_b = -8(d_1+d_2+d_3)(d_1^2+d_2^2+d_3^2)+20(d_1+d_2+d_3)(d_1d_2+d_2d_3+d_1d_3)-108d_1d_2d_3$.

If $\sigma_b > 0$, then $b \to +\infty$ as $k \to \infty$. Hence, by equation (3.2.26), it follows that $p > 0$ after a certain value of k. By factorizing d_2^3 from σ_b, it follows that $\sigma_b = d_2^3 \sigma$. Since $d_2 > 0$, condition $\sigma_b > 0$ is equivalent to condition (3.2.25). $\diamondsuit$

In the range between k_1 and k_2, the wave phenomena presented in Turing Theory may commit the cells with chemical concentrations close to the values of the associated steady state to become neurons. The constants k_T, x_1 and x_2 are dependent upon diffusion ratios D_1 and D_2. This shows that the conditions (3.2.24) and (3.2.25) are dependent on both diffusion ratios, which may impose more limitations in comparison with (3.1.29) and (3.1.30).

3.3 Results of the linear stability analysis

This section summarizes the analysis provided in the last two sections. The main results are as follows:

1. In the framework of Turing theory, there is a high potential for pattern formation and consequently for neuronal differentiation for the cells having the values close to the components of the steady states with Turing instability. Numerical results show that in the steady states with Turing instability, the level of Notch activity is low while the level of RA concentration is very high. For example for $\epsilon = 0$ and $\alpha = 0.5700$, $(u_0, v_0, w_0, q_0) = (1.7544, 0.0645, 2.8887, 1.7544)$ and for $\epsilon = 0.1$ and $\alpha = 0.5800$ $(u_\epsilon, v_\epsilon, w_\epsilon, q_\epsilon) = (1.7150, 0.0910, 2.0586, 1.7150)$.

2. By changing the parameter value α, the unperturbed system may exhibit different ranges of unstable waves. Fig. 3.1 is the plot of the largest of the eigenvalues $\lambda(k^2)$ for several values of parameter α. The system admits Turing-type patterns when $0.3625 < \alpha < 0.58$. For each value of α in the interval

(0.3625,0.58), there is a range of unstable wave numbers which is the interval on k^2 axis with positive values of $Re(\lambda)$.

3. In the absence of RA-Notch interaction, the following conditions are necessary and sufficient for axon formation: (3.1.10), (3.1.11), (3.1.29) and (3.1.30). In the presence of RA-Notch interaction, the following conditions are necessary and sufficient for axon formation: (3.2.13), (3.1.11), (3.2.24) and (3.2.25). For $\epsilon = 0$, the sufficeint conditions for Turing instability are only related to diffusion ratio $D_1 = \frac{d_3}{d_2}$, while for $\epsilon > 0$, they are dependent on both diffusion ratios $D_1 = \frac{d_3}{d_2}$ and $D_2 = \frac{d_1}{d_2}$.

4. Numerical results reveal that perturbation by RA-Notch interaction is restrictive on the steady states with Turing instability. Figure 3.3 is the plot of Turing instabilities for different values of $\epsilon > 0$. As $\epsilon \to 0$, pattern formation may happen in a wider range of α. In fact, the conditions (3.2.24) and (3.2.25) are dependent to both diffusion ratios which may impose more limitations in comparison with (3.1.29) and (3.1.30).

5. Equations (3.1.1)-(3.1.4) can be written in the form $\frac{dX}{dt} = F(\alpha, \epsilon, X) + D\nabla^2 X$ where $X = (u, v, w, q)$ and $\epsilon \geq 0$ is the perturbation parameter and $\alpha \in (0, 1)$ is the bifurcation parameter. Steady states of the system are represented by $X(\alpha, \epsilon)$ where all components of $X(\alpha, \epsilon)$ must be positive. For $\epsilon > 0$ small enough, the perturbed system may be topologically equivalent to the unperturbed system. This will be discussed in the following chapter.

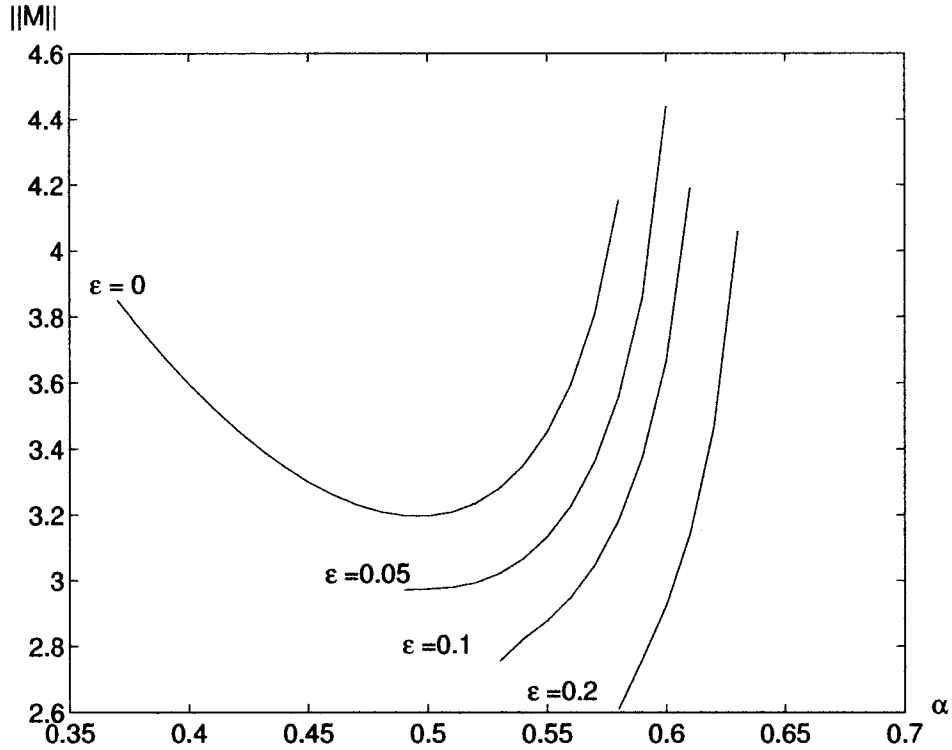

Figure 3.3 Plot of Turing instabilities for different values of $\epsilon > 0$ *where* $\|M\|$ *represents the Euclidean norm of the steady states with Turing instability. As* $\epsilon \to 0$ *the pattern formation may happen in a wider range of* α.

Chapter 4

Perturbation Analysis of RA-Notch Interaction

4.1 The Effects of RA-Notch Interaction on the Linear Stability of the Steady States

In this section, perturbation techniques are used to investigate the effects of small RA-Notch interaction on the linear stability of the steady states when $\epsilon \to 0$. Without considering spatial variations (i.e. $k = 0$), the eigenvalues of the linearized system of equations (2.10)-(2.13) are obtained by solving

$$|A_\epsilon - \lambda_\epsilon I| = 0. \tag{4.1.1}$$

Each eigenvalue is uniquely represented in the form of the perturbation series

$$\lambda_\epsilon = \lambda_o + \lambda_1 \epsilon + ..., \tag{4.1.2}$$

where $\lambda_o, \lambda_1, ...$ are known constants. The determinant (4.1.1) is equivalent to

$$(\lambda_\epsilon + a_4\gamma_4)P_3(\lambda_\epsilon), \tag{4.1.3}$$

where $P_3(\lambda_\epsilon)$ is a polynomial of degree three defined in (3.2.2). So, the first eigenvalue of the linearized system is

$$\lambda_\epsilon^{(1)} = -a_4\gamma_4. \tag{4.1.4}$$

Comparing this with unperturbed eigenvalues obtained in Section 3.1 of Chapter 3, one can simply observe that

$$\lambda_\epsilon^{(1)} = \lambda_o^{(1)} = -a_4\gamma_4 < 0. \tag{4.1.5}$$

This means that one of the eigenvalues is not perturbed at all. The leading order of the other three eigenvalues are defined by

$$\lambda_o^{(2)} = \gamma_1 f_{u_o} = -\gamma_1 a_1, \tag{4.1.6}$$

$$\lambda_o^{(3)}, \lambda_o^{(4)} = \frac{1}{2}\left\{(\gamma_2 g_{v_o} - \gamma_3 a_3) \pm \sqrt{(\gamma_2 g_{v_o} - \gamma_3 a_3)^2 + 4\gamma_2\gamma_3(a_3 g_{v_o} + y_{w_o} z_{v_o})}\right\}. \tag{4.1.7}$$

The effect of the perturbation on the stability of the steady states is considerable only if the real part of the leading order of an eigenvalue is zero (i.e. $Re(\lambda_o) = 0$). Clearly $\lambda_o^{(2)}$ is always real negative, but $Re(\lambda_o^{(3)})$ or $Re(\lambda_o^{(4)})$ may become zero if either

$$Q_o \equiv a_3 g_{v_o} + y_{w_o} z_{v_o} = 0 \tag{4.1.8}$$

or

$$P_o \equiv \gamma_2 g_{v_o} - a_3\gamma_3 = 0. \tag{4.1.9}$$

Hence, there are two possible cases for linear stability:

1. Conditions (4.1.8) and $P_o < 0$ imply that one of the eigenvalues is zero, i.e. $\lambda_o^{(3)} = 0$ and $\lambda_o^{(4)} = P_o$.

2. Conditions (4.1.9) and $Q_o < 0$ imply that there is a pair of pure imaginary eigenvalues, i.e.

$$\lambda_o^{(3),(4)} = \pm 2i\sqrt{-\gamma_2\gamma_3 Q_o}. \tag{4.1.10}$$

The steady state (u_o, v_o, w_o, q_o) for case 1 is often referred to as a multiple steady state. With the given parameters and coefficients, this will be a saddle-node steady state that is illustrated in Chapter 5. Case 2 represents a Hopf bifurcation at the steady state (u_o, v_o, w_o, q_o). With either of these two cases, the unperturbed steady state (u_o, v_o, w_o, q_o) is never asymptotically stable (and in the best case it is only stable). But the question is whether or not the perturbed steady state $(u_\epsilon, v_\epsilon, w_\epsilon, q_\epsilon)$ is asymptotically stable. The answer to this question can be determined by the real part of the next leading order of $\lambda_\epsilon^{(3)}$ in case 1 (or $\lambda_\epsilon^{(3),(4)}$ in case 2).

For case 1, substitute $\lambda_\epsilon^{(3)} = \epsilon\lambda_1^{(3)} + \epsilon^2\lambda_2^{(3)} + ...$ in the polynomial (3.2.2) which is defined in Section 3.2, Chapter 3. Note that the coefficients of this polynomial are perturbed so that each coefficient can be written in the form of the perturbation series

$$a_j = a_j^o + a_j^1\epsilon + ..., \tag{4.1.11}$$

for $j = 1, 2, 3$.

Then the polynomial (3.2.2) is rewritten as

$$P_3(\lambda^{(3)}) = (a_2^o \lambda_1^{(3)} + a_3^1)\epsilon + ... = 0. \tag{4.1.12}$$

The polynomial is zero if all coefficients of the series are zero. Since a_2^0 and a_3^1 are real values,

$$Re(\lambda_1^{(3)}) = -\frac{a_3^1}{a_2^o}. \tag{4.1.13}$$

From (3.33), (3.40) and (3.41), a_2^o can be written in the form

$$a_2^o = -h_1 P_o - \gamma_2 \gamma_3 Q_o. \tag{4.1.14}$$

Since h_1 is always positive, the conditions (4.8) and $P_o < 0$ imply that

$$a_2^o = -h_1 P_o > 0. \tag{4.1.15}$$

Therefore $Re(\lambda_1)$ does not blow up. Then the sign of λ_1 is crucial in determining the stability of the steady state. Let $a_3^1 > 0$, then $Re(\lambda_\epsilon^{(3)}) = \epsilon Re(\lambda_1^{(3)}) + ... < 0$. Since the other eigenvalues of the linearized system have negative real parts, the steady state $(u_\epsilon, v_\epsilon, w_\epsilon, q_\epsilon)$ is asymptotically stable. As $\epsilon \to 0$, this steady state may remain stable but it is no longer asymptotically stable (since $\lambda_o^3 = 0$). For example $\alpha = 0.77$ and $\epsilon = 0.02$ result in the homogeneous steady state $(u_\epsilon, v_\epsilon, w_\epsilon, q_\epsilon) = (1.2906, 0.8149, 17.4473, 1.2906)$ that is asymptotically stable, but its leading order $(u_o, v_o, w_o, q_o) = (1.2987, 0.7808, 16.0341, 1.2987)$, which corresponds to the steady state of the unperturbed system, is only stable.

For case 2, let us note the related eigenvalues with λ_ϵ; then $\lambda_\epsilon = \lambda_o + \lambda_1 \epsilon + ...$

is the perturbation series for the third and fourth eigenvalues where λ_o has been determined in (4.1.10). Obviously $Re(\lambda_o) = 0$; for the purpose of obtaining the real part of the next leading order, substitute λ_ϵ in the polynomial (3.32). Then

$$O(\epsilon^1) : 3\lambda_o^2\lambda_1 + 2a_1^o\lambda_o\lambda_1 + a_2^o\lambda_1 + a_1^1\lambda_o^2 + a_2^1\lambda_o + a_3^1 = 0. \tag{4.1.16}$$

The real and imaginary parts of $O(\epsilon^1)$ must be zero. Hence

$$Re(\lambda_1) = \frac{-(2a_1^o\lambda_o \mathrm{Im}(\lambda_1) + a_1^1\lambda_o^2 + a_3^1)}{3\lambda_o^2 + a_2^o}, \tag{4.1.17}$$

$$\mathrm{Im}(\lambda_1) = \frac{-(2a_1^o\lambda_o Re(\lambda_1) + a_2^1\lambda_o)}{3\lambda_o^2 + a_2^o}. \tag{4.1.18}$$

Equation (4.1.10) and $Q_o < 0$ imply that $\lambda_o^2 > 0$. Hence, $Re(\lambda_1)$ and $\mathrm{Im}(\lambda_1)$ do not blow up. Similar to case 1, if

$$2a_1^o\lambda_o \mathrm{Im}(\lambda_1) + a_1^1\lambda_o^2 + a_3^1 > 0, \tag{4.1.19}$$

then the perturbed steady state is asymptotically stable while the unperturbed steady state in the best case is just stable.

This is remarkable in two important respects. First, there is a qualitative change to the solution curves (trajectories) near the steady state as $\epsilon \to 0$. In this case this means that the perturbed and unperturbed system cannot be topologically equivalent near the steady state. Second, the necessary condition for Turing instability is that the steady state must be *asymptotically* stable, not just stable. Here the perturbed steady state is asymptotically stable while the unperturbed steady state is simply stable.

This raises the question of whether there is a case wherein the perturbed steady

state has the properties of Turing instability while the unperturbed steady state can not exhibit Turing instability. To answer this question it is necessary to know whether the steady state $(u_\epsilon, v_\epsilon, w_\epsilon, q_\epsilon)$ is unstable to spatial variation. Following the same steps taken in Section 3.2 of Chapter 3, $P_3(\lambda_\epsilon)$ is in the form of (3.2.11), i.e.

$$P_3(\lambda_\epsilon) = (\lambda_\epsilon + r)(\lambda_\epsilon^2 + p\lambda_\epsilon + q), \tag{4.1.20}$$

where $q > 0$ for all $k \geq 0$.

If $p < 0$ for some bounded interval of k, then the perturbed steady state is unstable to spatial variations. This is a required condition for Turing instability. p as a function of k is defined in the form

$$p = -P_o - \gamma_1 f_u + (d_1 + d_2 + d_3)k^2 - r, \tag{4.1.21}$$

where $P_o = \gamma_2 g_{v_o} - a_3\gamma_3$ and $-r$ is one of the perturbed eigenvalues.

Let $-r = \lambda_o + \epsilon\lambda_1 + ...$ For case 1, there are three possibilities for λ_o: either it is zero or P_o or $-\gamma_1 f_{u_o}$. So, the term (4.1.21) can be written in the form

$$p = (d_1 + d_2 + d_3)k^2 + \Gamma + \epsilon\lambda_1 + ..., \tag{4.1.22}$$

where $\Gamma > 0$.

For case 2, note that $-r$ is a real root of $P_3(\lambda_3)$and it can only be equal to $-\gamma f_{u_o}$. Hence in both cases for $\epsilon > 0$ small enough, $p \geq 0$ for all $k \geq 0$. This implies that $Re(\lambda(k)) \leq 0$, and therefore the condition for instability to spatial variations, is not satisfied and the perturbed system cannot exhibit Turing instability.

This is a significant result of perturbation analysis of the system showing that the perturbation by RA-Notch interaction cannot increase the number of steady

states with Turing instability. This means that if the unperturbed steady state does not have the properties of Turing instability, then the perturbed steady state does not either. Furthermore, it has been numerically confirmed that in the presence of RA-Notch interaction (i.e. $\epsilon > 0$), Turing instabilities occur for a fewer number of steady states (see Figure 3.3 in Chapter 3).

4.2 Conditions for perturbed and unperturbed systems to be topologically equivalent

The aim of this section is to illustrate that under some conditions the perturbed and unperturbed systems will perform the same qualitative structures near the perturbed and unperturbed steady states. In other words, the two systems will be topologically equivalent in a neighborhood of the related steady states. Before proving the equivalency between the two systems, let us define some mathematical terms in the following.

Definition 4.1: Let X be a metric space and let U and V be subsets of X. A *homeomorphism* of U onto V is a continuous one-to-one map of U onto V, $h : U \to V$, such that $h^{-1} : V \to U$ is continuous.

Definition 4.2: Consider two autonomous systems of differential equations such as

$$\dot{\mathbf{x}} = \mathbf{f}(\mathbf{x}), \tag{4.2.1}$$

and

$$\dot{\mathbf{x}} = g(\mathbf{x}), \tag{4.2.2}$$

where $x \in \mathbb{R}^n$ and with f, g vector fields.

The system (4.2.1) in a neighborhood of $p \in \mathbb{R}^n$ is topologically equivalent to the system (4.2.2) in a neighborhood of $q \in \mathbb{R}^n$ if there is a homeomorphism H mapping an open set U containing p onto an open set V containing $q = H(p)$ which maps trajectories of (4.2.1) in U onto trajectories of (4.2.2) in V and preserves their orientation by time in the sense that if a trajectory is directed from $\mathbf{x}_1$ to $\mathbf{x}_2$ in U, then its image is directed from $H(\mathbf{x}_1)$ to $H(\mathbf{x}_2)$ in V. If the homeomorphism H preserves the parameterization by time, then system (4.2.1) in a neighborhood of p is said to be *topologically conjugate* to system (4.2.2) in a neighborhood of q (see [37] for more details).

Definition 4.3: A steady state of a system of differential equations is said to be *hyperbolic* if all the eigenvalues of its Jacobian matrix have nonzero real parts ([17] for example).

Consider now two linear systems $\dot{x} = Ax$ and $\dot{x} = Bx$, $x \in \mathbb{R}^n$,

all of whose eigenvalues have nonzero real parts. Let m_- denote the number of eigenvalues with a negative real part and m_+ the number with a positive real part, so that $m_- + m_+ = n$.

The following theorem establishes the topological equivalency of linear systems:

Theorem 4.2. A necessary and sufficient condition for topological equivalence of two linear systems, all of whose eigenvalues have nonzero real parts, is that the number of eigenvalues with negative (and hence positive) real parts be the same in

both systems:

$$m_-(A) = m_-(B), m_+(A) = m_+(B) \tag{4.2.3}$$

The proof of this Theorem can be found in the book by V. I. Arnold [2]. One of the most interesting theorems in the theory of differential equations is the Hartman-Grobman Theorem which shows that in a neighborhood of a hyperbolic steady state, a system of differential equations is topologically equivalent to its linearization in a neighborhood of origin.

Theorem 4.1 (Hartman-Grobman Theorem). Let E be an open subset of $\mathbb{R}^n$ containing the point $x_p \in \mathbb{R}^n$, let $\mathbf{f} \in C^1(E)$, and let ϕ_t be the flow of the nonlinear system (4.2.1). Suppose that x_p is the hyperbolic steady state of the system (4.2.1) ($\mathbf{f}(\mathbf{x}_p) = 0$ and that the matrix $A = D\mathbf{f}(\mathbf{x}_p)$ has no eigenvalue with zero real part). Then there exists a homeomorphism H of an open set U containing x_p onto an open set V containing $H(x_p) = 0$ such that for each $y \in U$, there is an open interval $I_0 \subset \mathbb{R}$ containing zero such that for all $y \in U$ and $t \in I_0$

$$H \circ \phi_t(y) = e^{At} H(y); \tag{4.2.4}$$

i.e., H maps trajectories of (4.2.1) near the origin onto trajectories of (4.2.2) near the origin and preserves the parameterization by time ([37],p.120). The proof of this theorem can be found in the book by Philip Hartman ([18],Chapter IX).
Consider the perturbed system of equations (2.3.3)-(2.3.6) in the form of

$$\frac{d\vec{X}_\epsilon}{dt} = F(\vec{X}_\epsilon, \epsilon, \alpha) + D\nabla^2 \vec{X}_\epsilon, \tag{4.2.5}$$

where D is the diagonal matrix of diffusion coefficients, $\epsilon > 0$ the perturbation

parameter and $\alpha \in (0,1)$ is the bifurcation parameter. Then the unperturbed system of equations (2.3.3)-(2.3.6) can be written in the form

$$\frac{d\vec{X}_o}{dt} = F(\vec{X}_o, 0, \alpha) + D\nabla^2 \vec{X}_o \,. \tag{4.2.6}$$

Let $\vec{P}_\epsilon = (u_\epsilon, v_\epsilon, w_\epsilon, q_\epsilon)$ and $\vec{P}_o = (u_o, v_o, w_o, q_o)$ be the steady states of the perturbed and unperturbed systems (4.2.5) and (4.2.6) in the absence of spatial variations (i.e. $F(P_\epsilon, \epsilon, \alpha) = 0$ and $F(P_o, 0, \alpha) = 0$ when $D = 0$). As explained in the previous chapter, in the absence of spatial variations (i.e. $D = 0$), systems (4.2.5) and (4.2.6) can be linearized about the steady states of perturbed and unperturbed systems (i.e. $\vec{P}_\epsilon$ and $\vec{P}_o$). Let

$$\vec{R}_\epsilon = \begin{pmatrix} u - u_\epsilon \\ v - v_\epsilon \\ w - w_\epsilon \\ q - q_\epsilon \end{pmatrix} \text{ and } \vec{R}_o = \begin{pmatrix} u - u_o \\ v - v_o \\ w - w_o \\ q - q_o \end{pmatrix}. \tag{4.2.7}$$

Then for $\left\|\vec{R}_\epsilon\right\|$ and $\left\|\vec{R}_o\right\|$ small, the systems (4.2.5) and (4.2.6) linearized about the steady states $\vec{P}_\epsilon$ and $\vec{P}_o$ are presented in the form

$$\frac{d\vec{R}_\epsilon}{dt} = A_\epsilon \vec{R}_\epsilon, \tag{4.2.8}$$

$$\frac{d\vec{R}_o}{dt} = A_o \vec{R}_o, \tag{4.2.9}$$

where A_ϵ and A_o are the Jacobian matrices of $F(\vec{X}_\epsilon, \epsilon, \alpha)$ and $F(\vec{X}_o, O, \alpha)$ at the fixed points $\vec{P}_\epsilon$ and $\vec{P}_o$.

The following proposition is established to pursue the study of the system perturbed by RA-Notch interaction.

Proposition 4.1

Let E be an open subset of $\mathbb{R}^4$ containing the steady states $\vec{P}_\epsilon$ and $\vec{P}_o$ of the systems (4.2.5) and (4.2.6) respectively, and let $F(\vec{X}_\epsilon, \epsilon, \alpha)$ and $F(\vec{X}_o, \epsilon, \alpha) \in C^1(E)$, then in the absence of spatial variation (i.e. $D = 0$), the system (4.2.5) in a neighborhood U_ϵ of $\vec{P}_\epsilon \in \mathbb{R}^n$ is topologically equivalent to the system (4.2.6) in a neighborhood U_o of $\vec{P}_o \in \mathbb{R}^n$ if the following conditions are satisfied:

1. The steady states $\vec{P}_\epsilon$ and $\vec{P}_o$ of the systems (4.2.5) and (4.2.6) are both hyperbolic.

2. $\epsilon > 0$ is small enough such that the real and imaginary parts of each eigenvalue λ_ϵ of A_ϵ have the same sign as the real and imaginary parts of the corresponding eigenvalue λ_o of A_o.

Proof.

The proof of this proposition is an immediate application of the Hartman-Grobman Theorem and Theorem 4.2.

Define $\phi_\epsilon : \mathbb{R} \times \mathbb{R}^4 \to \mathbb{R}^4$ the flow of the system (4.2.5). It then follows from the Hartman-Grobman Theorem that there exists a homeomorphism h_ϵ of an open set U_ϵ containing the origin onto an open set V_ϵ containing the origin such that $h_\epsilon(P_\epsilon) = 0$ and for each $y_\epsilon \in U_\epsilon$ there is an open interval $I_\epsilon \subset \mathbb{R}$ containing zero such that for all $y_\epsilon \in U_\epsilon$ and $t \in I_\epsilon$

$$h_\epsilon \circ \phi_\epsilon(t, y_\epsilon) = e^{A_\epsilon t} h_\epsilon(y_\epsilon). \tag{4.2.10}$$

Similarly, the system (4.2.6) in a neighborhood U_o of $\vec{P}_o \in \mathbb{R}^n$ is topologically conjugate to its linearized form (4.2.9) in a neighborhood of the origin; i.e. there exists a homeomorphism h_o which maps trajectories of (4.2.6) near the steady state $\vec{P}_o$ onto trajectories of (4.2.9) near the origin and preserves the parameterization by time. Since the systems (4.2.5) and (4.2.6) are topologically equivalent to their linearized form, it is only required to show that the two linearized systems (4.2.8) and (4.2.9) are topologically equivalent.This can be done by implementing the Theorem 4.2. From conditions 1 and 2 of this proposition one can simply observe that the hypotheses of the Theorem 4.2 are satisfied.Diagram (4.2.11) schematizes the topological equivalency of the systems (4.2.5) and (4.2.6) under the homeomorphism $H = h_o^{-1} \circ h_L \circ h_\epsilon$.

$$\begin{array}{ccc} \dfrac{d\vec{X}_\epsilon}{dt} = F(\vec{X}_\epsilon, \epsilon, \alpha) & \xrightarrow{H} & \dfrac{d\vec{X}_o}{dt} = F(\vec{X}_o, 0, \alpha) \\ h_\epsilon \downarrow & & h_o \downarrow\uparrow h_o^{-1} \\ \dfrac{d\vec{R}_\epsilon}{dt} = A_\epsilon \vec{R}_\epsilon & \xrightarrow{h_L} & \dfrac{d\vec{R}_o}{dt} = A_o \vec{R}_o \end{array} \tag{4.2.11}$$

Diagram:(4.2.11) *Under the hypothesis of Proposistion 4.1, two perturbed and unperturbed systems is topologically equivalent with the homeomorphism* $H = h_o^{-1} \circ h_L \circ h_\epsilon$.

The homeomorphisms $h_\epsilon : U_\epsilon \to V_\epsilon$ and $h_o : U_o \to V_o$ are already defined by the Hartman-Grobman Theorem and the homeomorphism h_L is defined by Theorem 4.2.$\Diamond$

It is important to note that the two systems (4.2.5) and (4.2.6) may not be topologically conjugate. For topological conjugacy it is necessary that the homeomorphism between the two systems preserve the parameterization by time. Here,

the homeomorphism $H = h_o^{-1} \circ h_L \circ h_\epsilon$ may notnecessarily preserve the parameterization by time. In the previous chapter, the method of eigenfunction expansion was employed to construct solutions to the initial boundary value problem (3.1.18)-(3.1.20)for the system linearized about the steady state. In the same way as shown in (3.1.25), the eigenfunctions for the perturbed and unperturbed systems satisfy

$$\frac{d\vec{W}_\epsilon}{dt} = (A_\epsilon - Dk^2)\,\vec{W}_\epsilon, \tag{4.2.12}$$

$$\frac{d\vec{W}_o}{dt} = (A_o - Dk^2)\,\vec{W}_o\,. \tag{4.2.13}$$

Similar to the proof of Proposition 4.1, it can be shown that the linear systems (4.2.12) and (4.2.13) are topologically equivalent if the real part and imaginary part of each eigenvalue $\lambda_\epsilon(k)$ of $A_\epsilon - k^2 D$ have the same sign as the real and imaginary parts of the corresponding eigenvalue $\lambda_o(k)$ of $A_o - k^2 D$.

Therefore, under hypothesis of Proposition 4.1 and the conditions for eigenvalues mentioned above in a neighborhood of the steady state with Turing instability, the perturbed and unperturbed system are topologically equivalent. The biological interpretation of this result is that under the hypotheses of Proposition 4.1, the small interactions between RA and Notch signaling pathways may not have a qualitative effect on either the symmetry breaking instabilities of the system or the process of axon formation.

Chapter 5

Bifurcations and Numerical Simulations

5.1 Bifurcations at the steady state

In Chapters 3 and 4, the mathematical model of axon formation was locally analyzed around the steady states of the system. Linear stability analysis and perturbation techniques were used to study the effects of external signals (RA and Notch) on the symmetry breaking instabilities for axon formation. In this section, the qualitative behavior of the system $\frac{d\vec{X}_\epsilon}{dt} = F(\vec{X}_\epsilon, \epsilon, \alpha)$ is numerically studied as the parameter α changes and $\epsilon \ll 1$. If the qualitative behavior of the system remains the same for all vector fields F of different ϵ and α parameter values, then the system is said to be structurally stable with respect to α and ϵ. Otherwise, the system has a set of bifurcations. Furthermore, near the steady states with Turing instability, the qualitative behavior of the system $\frac{d\vec{X}}{dt} = F(\vec{X}, \epsilon, \alpha) + D\nabla^2 \vec{X}$ may change with different values of diffusion coefficients of the system. This is a certain type of bifurcation which is called a Turing bifurcation. The Turing bifurcation is the

basic idea for generation of spatial patterns which can be found in most of the mathematical models for biological pattern formation (see [16] for more details).

In this study, the Turing bifurcation may occur when there are changes to the diffusion ratios $D_1 = \frac{d_1}{d_2}$ (and $D_2 = \frac{d_3}{d_2}$) while the other types of bifurcation may happen for the spatially homogeneous system (i.e. $d_i = 0$ for $i = 1, .., 4$) when the parameter α passes through a bifurcation value α_o with $\epsilon \ll 1$.

Consider the system of equations (3.1.1)-(3.1.4). The first step in studying the bifurcations of the system is to find the bifurcations by the parameter $\alpha \in (0, 1)$ when $\epsilon \ll 1$. By setting the coefficients of the system (3.1.1)-(3.1.4) to the same values taken in Section 3.1 of Chapter 3, the homogeneous system of equations may have various types of steady states for $\alpha \in (0, 1)$ and $\epsilon \ll 1$. Numerical results reveal that the system becomes structurally unstable for parameter values of $\alpha_1 = 0.3625$ and $\alpha_2 = 0.58$. This means that the behavior of the system changes as the parameter α passes through α_1 and α_2.

For each $\alpha < \alpha_1$, the homogeneous system has a pair of steady states, which are a saddle and a stable node. For $\alpha \in (\alpha_1, \alpha_2)$, the number of the steady states will change to four, so that there are two pairs of saddles and stable nodes. For each $\alpha \in (\alpha_2, 1)$, the system returns to a pair of saddle and stable node steady states. As α approaches to one, these two steady states merge and create an unstable saddle-node steady state such that the behavior of the system changes at $\alpha_3 = 1$.

The components of the steady states of the homogeneous system can be written as functions of the level of Notch activity; i.e. the steady state $(u_\epsilon, v_\epsilon, w_\epsilon, q_\epsilon) = (\xi_1(v_\epsilon), v_\epsilon, \xi_2(v_\epsilon), \xi_3(v_\epsilon))$, where

$$\xi_1(v_\epsilon) = \frac{1}{\alpha a_1} - \frac{\epsilon}{a_1} v_\epsilon, \tag{5.1.1}$$

$$\xi_2(v_\epsilon) = \frac{1}{a_3(1 + c_3 v_\epsilon^2)}, \tag{5.1.2}$$

$$\xi_3(v_\epsilon) = \frac{1}{a_4}\xi(v_\epsilon), \tag{5.1.3}$$

and v_ϵ is a root of the polynomial

$$P_4(v_\epsilon, \epsilon, \alpha) = (c_2 a_3^2(1 + c_3 v_\epsilon^2)^2 + 1)(\frac{a_2}{(\alpha - 1)}(v_\epsilon - \alpha)^2 + \epsilon\xi_1(v_\epsilon) + 1). \tag{5.1.4}$$

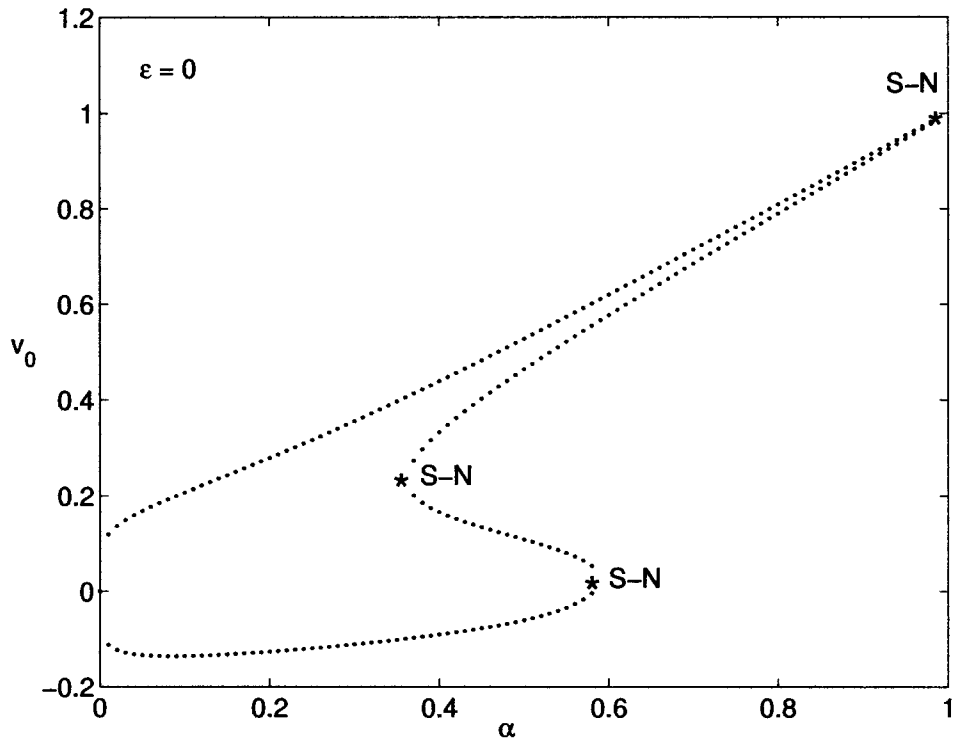

Figure 5.1 *The bifurcation diagram corresponding to the homogeneous system (3.1.1)-(3.1.4) when* $\epsilon = 0$. $\alpha_1 = 0.3625$, $\alpha_2 = 0.58$ *and* $\alpha_3 = 1$ *are the saddle-node bifurcation (S-N) values of the system (shown with * in the figure).*

Since u_ϵ, w_ϵ and q_ϵ are functions of v_ϵ, the multiplicity and the position of the steady state $(u_\epsilon, v_\epsilon, w_\epsilon, q_\epsilon)$ is determined by the number and the values of the roots of $P_4(v_\epsilon, \epsilon, \alpha)$. Hence, the qualitative changes of the unperturbed homogeneous system (3.1.1)-(3.1.4) can be illustrated by plotting the steady states of the one-dimensional system $\frac{dv_o}{dt} = P_4(v_o, 0, \alpha)$. Figure 5.1 shows the bifurcation diagram corresponding to the homogeneous system (3.1.1)-(3.1.4) when $\epsilon = 0$. The values $\alpha_1 = 0.3625$ and $\alpha_2 = 0.58$ are the saddle-node bifurcation values of the system. The third saddle-node bifurcation may occur at $\alpha_3 = 1$, but one should note that α_3 is not within the designated range for $\alpha \in (0, 1)$.

The bifurcation diagram with respect to α has an overlapping branch which is shown in Figure 5.1. Numerical results show that the steady states of the homogeneous system (3.1.1)-(3.1.4) corresponding to this branch are the only steady states which may have the properties of Turing instability. Generally, α and the diffusion ratio $D_1 = \frac{d_3}{d_2}$ are two important parameters that distinguish the steady states with Turing instability from the other steady states of the unperturbed system (3.1.1)-(3.1.4). The diffusion ratio $D_1 = \frac{d_3}{d_2}$ determines whether or not the steady states related to the overlapped branch have the properties of Turing instability. For each $\alpha \in (\alpha_1, \alpha_2)$, when the parameter D_1 passes through a critical value $D_c^{(1)}$, the qualitative behavior of the solution set of the inhomogeneous system (3.1.1)-(3.1.4) will change and the steady state corresponding to the overlapped branch becomes spatially unstable. This corresponds to the Turing bifurcation and the critical value $D_c^{(1)}$ is a bifurcation value for the system; i.e. for $D_1 > D_c^{(1)}$, the steady state has Turing properties while for $D_1 < D_c^{(1)}$ it is spatially stable.

Numerical simulations of the system gives valuable insight into the behavior of the unperturbed system of equations.

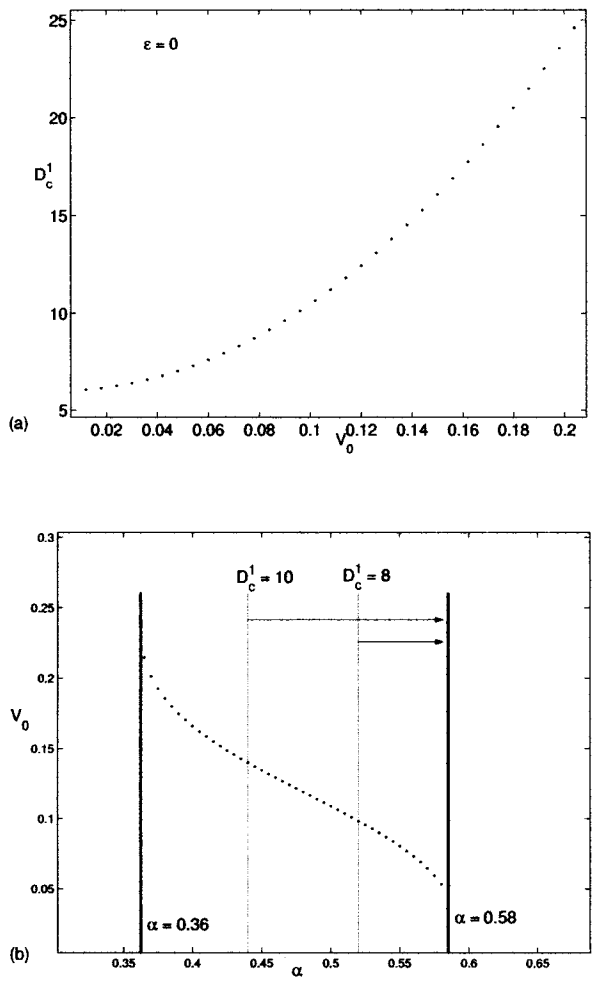

Figure 5.2 *(a) Plot of the bifurcation values of the unperturbed system (i.e. $\epsilon = 0$) for the values of Notch activities (v_o) of the steady state (u_o, v_o, w_o, q_o) corresponding to the overlapped branch.*

(b) By decreasing the value of D_1, the Turing instability occurs in a shorter range of α. As D_1 tends toward a critical value near 6, the system has no steady states with Turing instability which means no axon formation or neuronal differentiation.

Figure 5.2(a) plots the bifurcation values of the unperturbed system (i.e. $\epsilon = 0$) for the values of Notch activities (v_o) of the steady state (u_o, v_o, w_o, q_o) corresponding to the overlapped branch. For $D_1 > 25$, each of these steady states has the properties of Turing instability and the system exhibits symmetry breaking for axon formation near these steady states. The biological interpretation of the bifurcation curve in Figure 5.2(a) is that axon formation and neuronal differentiation might be possible for the cells with a higher level of Notch only if Delta diffuses (in terms of signal transduction) faster than Notch. However, one should note that there is a threshold for the level of Notch activity. With the given constants and parameters in this study, no axon formation is expected for v_o greater than 0.23.

As mentioned before, Turing instability is possible only for the steady states with the lowest level of Notch activity (i.e. v_o) in the range of $\alpha \in (0.3625, 0.58)$. This means that the steady states with Turing instability are trapped between two saddle node bifurcations at α_1 and α_2. This is remarkable when changing the value of the diffusion ratio D_1 results in decreasing the number of steady states with Turing instability. Figure 5.2(b) shows that by decreasing the value of D_1, the Turing instability occurs in a shorter range of α. As D_1 tends toward a critical value near 6, the system has no steady states with Turing instability which means no axon formation or neuronal differentiation. This shows the importance of diffusion ratio D_1 for the symmetry breaking instabilities of the system.

So far the numerical results presented in this section are for the case in which the system is unperturbed. When $\epsilon > 0$ is small enough (i.e. $\epsilon \ll 1$ such that the eigenvalues related to the linearized system preserve their signs as the system is perturbed), by Proposition 4.1 no qualitative change to the steady states of the homogeneous system (3.1.1)-(3.1.4) is expected. Figure 5.3 shows the bifurcation diagrams of the one-dimensional system $\frac{dv_\epsilon}{dt} = P_4(v_\epsilon, \epsilon, \alpha)$ corresponding to

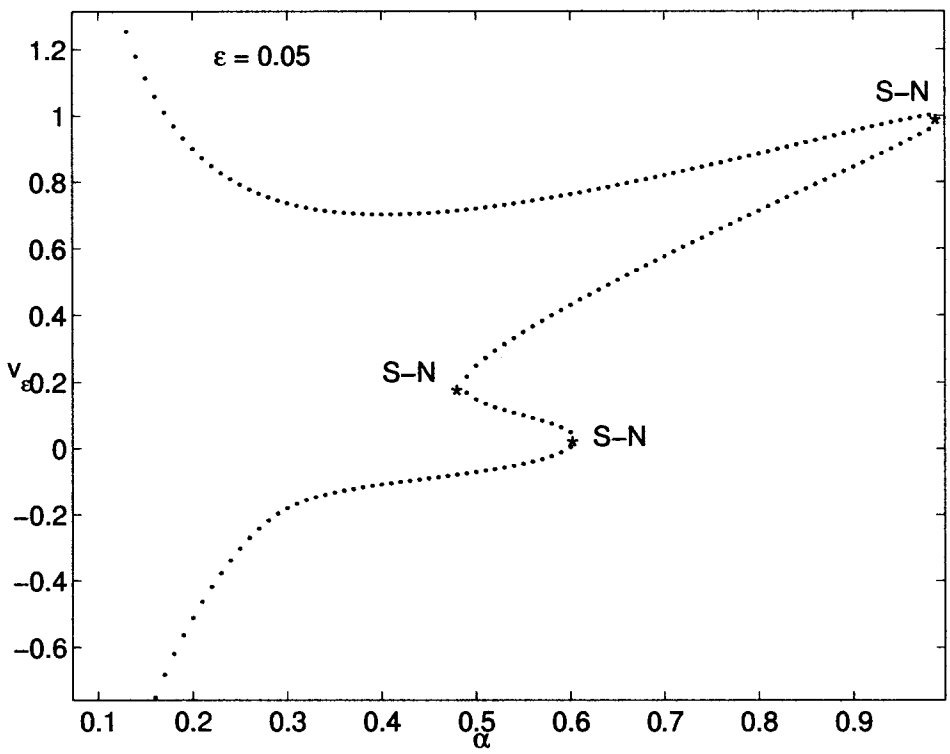

Figure 5.3 *The bifurcation diagram of the one-dimensional system* $\frac{dv_\epsilon}{dt} = P_4(v_\epsilon, \epsilon, \alpha)$ *corresponding to the homogeneous perturbed system (3.1.1)-(3.1.4) for* $\epsilon = 0.05$ *and in the absence of spatial variation. There are still three saddle-node steady states (shown with * in the figure)*

the homogeneous perturbed system (3.1.1)-(3.1.4) for $\epsilon = 0.05$ and in the absence of spatial variation. Numerical results show that in this case there are still three saddle-node steady states and the stability of the steady states of the system remains unchanged after perturbation. The next section confronts the case in which the perturbation by RA-Notch is remarkably large (i.e. the condition $\epsilon \ll 1$ is removed and $\epsilon > 0$ can be arbitrarily large).

5.2 Transformation of the saddle-node bifurcations to Hopf bifurcations

This section addresses the question of how the qualitative behavior of the system (3.1.1)-(3.1.4) changes as the perturbation by RA-Notch interaction increases remarkably. The numerical study of the homogeneous system shows that by increasing the parameter value $\epsilon > 0$, there is a transformation of saddle-node bifurcations into Hopf bifurcations. A saddle-node bifurcation occurs at a non-hyperbolic steady state where the Jacobian matrix of linearization (i.e. A_ϵ) has an eigenvalue with zero real part. By increasing the value of $\epsilon > 0$, the saddle-node steady state transforms to a steady state with the Jacobian linearization matrix that has a pair of purely imaginary eigenvalues and no other eigenvalues with zero real part. Similar to the previous section, the qualitative changes of the homogeneous system (3.1.1)-(3.1.4) can be illustrated by plotting $P_4(v_\epsilon, \epsilon, \alpha) = 0$. Figure 5.4 shows the bifurcation diagram corresponding to the homogeneous system when $\epsilon = 0.5$. The saddle-node bifurcations at $\alpha_1 = 0.3625$ and $\alpha_2 = 0.58$ have been transformed to the Hopf bifurcations at $\alpha_{1'} = 0.64$ and $\alpha_{2'} = 0.6752$ while the third bifurcation at $\alpha_3 = 1$ is still a saddle-node bifurcation.

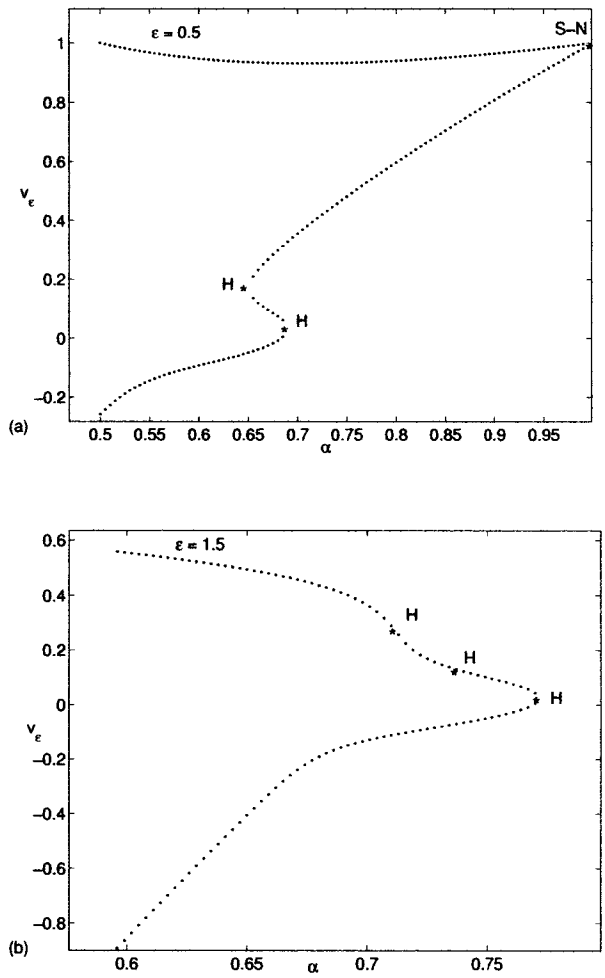

Figure 5.4 *(a) The saddle-node bifurcations (S-N) at* $\alpha_1 = 0.3625$ *and* $\alpha_2 = 0.58$ *have been transformed to the Hopf bifurcations (H) at* $\alpha_{1'} = 0.64$ *and* $\alpha_{2'} = 0.6752$ *while the third bifurcation at* $\alpha_3 = 1$ *is still a saddle-node bifurcation (S-N).*

(b) All saddle-node bifurcations (S-N) have vanished and instead Hopf bifurcations (H) have appeared. Turing instabilities occur for the steady states between $\alpha_{1''} = 0.725$ *and* $\alpha_{2''} = 0.741$.

Similar to the unperturbed case, the steady states corresponding to the overlapped branch (shown in Figure 5.4(a)) may have the properties of Turing instability, but here there are two diffusion ratios $D_1 = \frac{d_3}{d_2}$ and $D_2 = \frac{d_1}{d_2}$ that determine whether or not these steady states have the properties of Turing instability. This is an important distinction to the unperturbed case where D_2 is not involved in determining this quality. By increasing the perturbation value to 1.5, the third saddle-node bifurcation point is transformed to the Hopf bifurcation. This is shown in Figure 5.4(b) where all saddle-node bifurcations have vanished and instead Hopf bifurcations have appeared. Furthermore, there is a stability change for some steady states of the system such that their linear stability has changed to an instability. Depending on diffusion ratios D_1 and D_2, the Turing instability may occur for the steady states between $\alpha_{1''} = 0.725$ and $\alpha_{2''} = 0.741$. Again the Turing bifurcation for each of these steady states depends on two parameters D_1 and D_2.

The Turing bifurcation is associated with the passage of a real eigenvalue through zero (steady-state bifurcation), and the Hopf bifurcation with the crossing of the imaginary axis by a complex-conjugate pair of eigenvalues. The coexistence of Turing and Hopf bifurcations in a system of reaction-diffusion equations is a considerable fact. Previous theoretical work [39],[35] has shown that the closer the system is to the Hopf bifurcation point, the more the Turing instability is generally favored. The value of the diffusion coefficient ratio for which Turing instability becomes possible moves closer to one (the realistic value for homogeneous systems), as the Hopf boundary is approached.

The interaction of Turing and Hopf bifurcation in chemical systems is of great interest since both bifurcations have been observed experimentally in a chloride-iodide-malonic acid (CIMA) reaction by varying the concentration of the color indicator in the reactor [11],[36]. Generally, when a Turing bifurcation occurs close to a

Hopf bifurcation in the parameter space of a reaction-diffusion system, the Turing and Hopf modes may interact nonlinearly to form a variety of complex spatiotemporal patterns. This type of interaction has been studied for different systems of reaction-diffusion equations [40]. However, this is beyond the scope of the present work. The analytical and numerical results of this work have also been experimentally investigated. The following chapter provides the results of these laboratory experimentations and imparts the final statements concerning this study.

Chapter 6

Biological Experiments and Conclusions

6.1 Experimental results

This section is a brief report of the laboratory experiments that have been carried out at the Institute for Biological Sciences (NRC), Ottawa, Ontario to explore the theoretical predictions of this study. See Appendix B for specific details about the method, cell culture, transfection and differentiation comprising the experiments. In the absence of the external signals, RA and Notch, most of the N2a cells remained undifferentiated such that axon formation occurred in almost none of the cells (Figure 6.1(a)). When Notch signals were added to the system, the negative feedback became weaker. Thus, in the absence of RA signals, no axon formation was expected (Chapter 3, Section 3.1). This has been confirmed in experiment in the case that only activated Notch was utilized. The red dots in Figure 6.1(b) represent the existence of saturated Notch in the N2a cells where they remained undifferentiated. (No axon formation occurred in any of them). A low concentration of RA with a

high level of activated Notch in the experiment resulted in few cell differentiations or axon formations. Figure 6.2(a) illustrates the cells when low concentration of RA (10^{-4} M) and activated Notch were added to the dish. An increase in the concentration of RA resulted in more cell differentiations and more axon formations. Figure 6.2(b) shows the case where the concentration of RA was increased to 10^{-2} M. Obviously, there are more neurons indicating more axon formations. Comparing this result to the case in which RA concentration was lower (10^{-4} M), Figure 6.2 (b) demonstrates that neurite outgrowth in the cells with saturated Notch (shown with red dots) increased.

Absence of Notch signals in the theory corresponds to the case in which the negative feedback is sufficiently strong. In this case, adding a high concentration of RA signals to the system was expected to produce a positive feedback stronger than the negative feedback such that the symmetry between the neurites would break and one of the neurites would become an axon(see chapter 2 section 2.1). Figure 6.3 represents the case that a high concentration of RA was added to the cells and no activated Notch was introduced to the system. This resulted in most of the cells differentiating to neurons which confirmed axon formation in most of the cells.

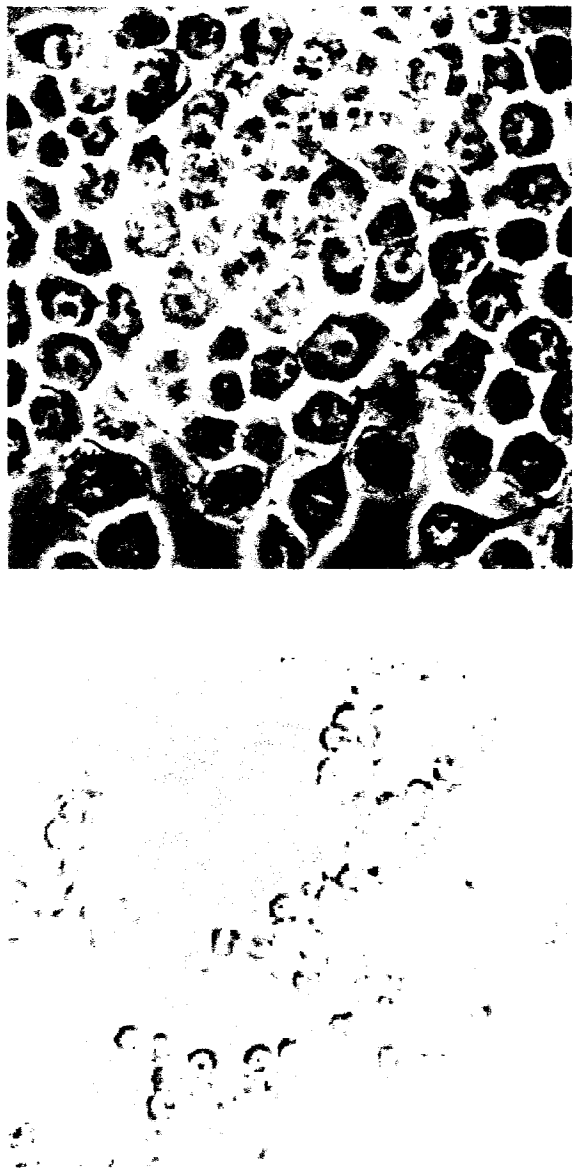

Figure 6.1 *(a) In the absence of the external signals, RA and Notch, most of the N2a cells remained undifferentiated such that axon formation occurred in almost none of the cells.*

(b) The case that only activated Notch is utilized: the red dots represent the existence of saturated Notch in the N2a cells where they remained undifferentiated (no axon formation occurred in any of them.)

Figure 6.2 *(a) Low concentration of RA (10^{-4} M) and activated Notch added to the dish resulted in few axon formations.*

(b) An increase in the concentration of RA ($10^{-2}M$ from $10^{-4}M$) resulted in more cell differentiations and more axon formations.

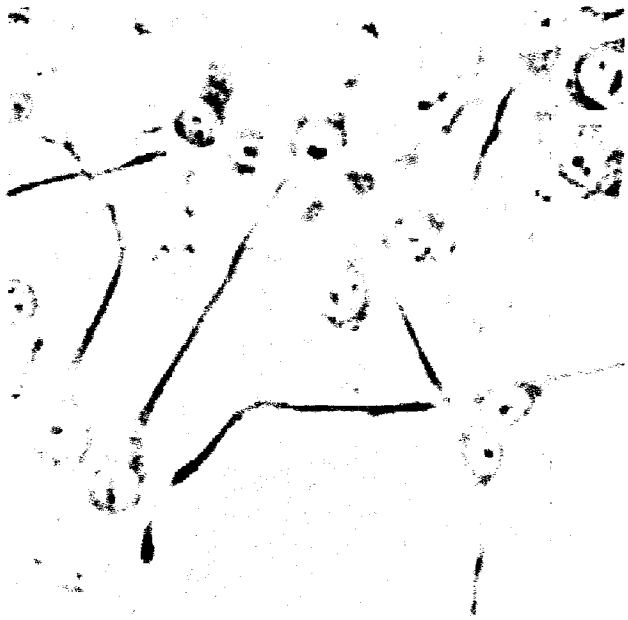

Figure 6.3 *The case that a high concentration of RA was added to the cells and no activated Notch was introduced to the system resulted in most of the cells differentiating to neurons which confirms axon formation in most of the cells.*

6.2 Conclusions

James D. Murray, the founder of the Centre for Mathematical Biology at the University of Oxford admonishes ([29], p.xi),

> *Biomedical science is clearly the premier science of the foreseeable future. For the continuing health of their subject, mathematicians must become involved with biology. With the example of how mathematics has benefitted from and influenced physics, it is clear that if mathematicians do not become involved in the biosciences they will simply not be a part of what are likely to be the most important and exciting scientific discoveries of all time.*

The complexity of the biological sciences demands new research tools to understand the key issues from a different perspective. As biology becomes more quantitative, mathematical biology research introduces itself as an imperative instrument while simultaneously opening new and energizing branches in mathematics.

The present work is an implementation of mathematical methods and techniques in one of the key issues in neurobiology at the cellular level. The proposed model is another example of inclusion of a network of signaling pathways into the Turing mechanism with the aim of studying the effects of external signals (RA and Notch1) on the symmetry breaking instabilities for axon formation. It is felt that one particular merit of the work presented here is that it shows the possible existing connection between feedback mechanism and Turing mechanism for the production of symmetry breaking instabilities. When activated Notch was utilized in the absence of RA, the cultured cells in the dish remained undifferentiated and there was no axon formation. This has been forecasted in the theoretical discussion (see Chapter 3, Section 3.1) where the general system is reduced to the Delta-Notch subsystem and

the negative feedback has been weakened by Notch external signals. In the absence of an RA signaling pathway, the positive feedback loop is not generated to provide a potential for neurites to become an axon. Hence, the cells with components of axon free steady states remain undifferentiated. Utilizing different concentrations of RA in the experiment corresponds to different values of α in the system. The linear stability analysis shows that Turing instability occurs for $\alpha \in (0.3625, 0.58)$. The concentration of RA utilized in the experiment is proportional to $\frac{1}{\alpha}$. Laboratory experimentations show that axon formation is possible in a range of concentrations for RA.

In theory, existence of Turing instability for the system corresponds to a high potential for axon formation and neuronal differentiation for the cells having the values close to the components of the steady states with Turing instability. Numerical results show that in the steady states with Turing instability, the level of Notch activity is the lowest while the level of RA concentration is very high (Chapter 3, Section 3.3). Experimental results confirm that high concentrations of RA with low levels of activated Notch lead to neuronal differentiation (axon formation).

Numerical results attest that perturbation by RA-Notch interaction is restrictive on the steady states with Turing instability. As $\epsilon \to 0$, the pattern formation may happen in a wider range of α (Figure 3.3). For the perturbed steady states, there are two diffusion ratios $D_1 = \frac{d_3}{d_2}$ and $D_2 = \frac{d_1}{d_2}$ that determine whether or not these steady states have the properties of Turing instability. The Turing bifurcation curve (Figure 5.2(a)) for the unperturbed system (3.1.1)-(3.1.4) suggests that axon formation and neuronal differentiation might be possible for the cells with a higher level of Notch only if Delta diffuses (in terms of signal transduction) faster than Notch. The numerical study of the homogeneous system shows that by increasing the parameter value $\epsilon > 0$, there is a transformation of saddle-node bifurcations into

Hopf bifurcations. The interaction of Turing and Hopf bifurcations may bring an insight to the mathematical study of axon formation and neuronal differentiation. Small perturbations of RA-Notch interaction may change the stability of the homogeneous steady states. A multiple steady state may change to an asymptotically stable steady state. But if the unperturbed steady state does not have the properties of Turing instability, then the perturbed steady state does not either. Under some conditions, the small perturbations do not change the qualitative behavior of the system and the perturbed and unperturbed systems are topologically equivalent (Chapter 4, Section 4.2). The biological interpretation of this result is that the small interactions between RA and Notch signaling pathways may not have a qualitative effect on either the symmetry breaking instabilities of the system or the process of axon formation.

The present work has studied the effects of external signals on the axon formation and neuronal differentiation in a model of reaction-diffusion equations. Future studies might include the interaction of Turing and Hopf bifurcations in the present system of equations which may produce some interesting results for the prediction of axon formation in N2a cells. Particularly, it might be possible to show that the coupling of Turing and Hopf bifurcation may result in periodic spatial symmetry breaking instabilities for axon formation.

Appendix A

Glossary of Biological Terms

axon

The threadlike extensions on a neuron, or nerve cell which conducts nerve impulses; the arm of a nerve cell that normally transmits outgoing signals from one cell body to another. Each nerve cell has one axon, which can be relatively short in the brain but can be up to three feet long in other parts of the body.

cell differentiation

A concept from developmental biology describing the process by which cells acquire a "type". The morphology of a cell may change dramatically during differentiation, but the genetic material remains the same, with few exceptions.

dendrite

Microscopic tree-like fibers extending from a neuron. They are receptors of electrochemical nervous impulse transmissions. This stimulation arrives through synapses, which typically are located near the tips of the dendrites and away from the cell body.

gene

The functional and physical unit of heredity passed from parent to offspring. Genes are pieces of DNA, and most genes contain the information for making a specific protein. Each of the body's 50,000 to 100,000 genes contains the code for a specific product, typically, a protein such as an enzyme.

morphogen

A substance that stimulates the development of form or structure in an organism.

morphogenesis

The process of differentiation of cells into different tissues or structures.

neurite

Any neuronal process (axon or dendrite). This term is typically used to refer to the processes of neurons in cell culture.

neuroblastoma cell

Neuroblastomas are fast-growing cancers that develop from nerve cells and typically arise in the adrenal glands.

neuron

Neurons are the nerve cells which make up the central nervous system. They consist of a nucleus, a single axon which conveys electrical signals to other neurons and a host of dendrites which deliver incoming signals.

Notch Signaling (Delta-Notch Signaling Pathway)

The Notch pathway is a conserved signaling pathway that controls cell fate during animal development. Notch serves as a receptor for direct cell-cell signaling by transmembrane proteins (e.g., Delta which serves as a ligand) on neighboring cells.

pattern formations

The developmental processes by which the complex shape and structure of higher organisms occurs

signaling pathway

A series of chemical reactions ending up in achieving cell movement (chemotaxis) and gene activation and some other cell functions. In gene activation, a particular signaling molecule turns on a certain gene in a cell and consequently, the genetic information encoded in DNA is converted into proteins. The concentration of these proteins and other chemical reactions result in developments in embryo such as cell division or cell differentiation or interaction with other cells to form tissues in the body.

signal transduction

Communication inside the cell, and also, how a cell reacts to an external signal by transmitting it across the cell membrane to the interior of the cell. Proteins on the cell surface function as receptors for specific molecules (such as the hormone, insulin). The binding of the molecule to the receptor initiates an interlinked series of biochemical events inside the cell, involving enzymes, proteins and ions.

Appendix B

Cell Culture, Transfection and Differentiation

Cell Culture: N2a neuroblastoma cells (ATCC, Manassas, VA) were plated at the density of 3 X 105 cells/ml in Dulbecco's Modified Eagle Medium (DMEM), high glucose, L-glutamine (Invitrogen Corporation, Burlington, ON) + 10 percent fetal bovine serum (FBS; Hyclone, Logan, UT). On the next day, cells were transiently transfected, as described below. In order to examine neuronal differentiation, cells were incubated in the presence of all-trans retinoic acid (RA, Sigma-Aldrich Ltd., Oakville, ON) for three days and examined for neurite outgrowth. Parallel cultures were also stained with neuronal markers [microtubule associated protein 2 (MAP2) or neurofliment 200 (NF200)] to ensure the neuronal identity of the cells.

Transient Transfection: N2a cells were incubated for 7 hours with 1 μ/ml of Notch1-ICD-dsRed2 plasmid DNA and 5μ/ml of Lipofectamine 2000 (Invitrogen), according to the manufacturer's instructions. Cells were rinsed with phosphate buffered saline (PBS), incubated in fresh medium (DMEM + 10 percent FBS) and examined for neurite outgrowth in the absence or presence of retinoic acid.

Bibliography

[1] S.S. Andersen and Guo-qiang Bi. Axon formation: a molecular model for the generation of neuronal polarity. *BioEssays*, 22:172-179, 2000.

[2] V. I. Arnold Ordinary Differential Equations chapter 3 page 143 MIT press 1973

[3] J.L. Aragon, M. Torres, D. Gil, R.A. Barrio, and P.K. Maini. Turing patterns with pentagonal symmetry. *Phys. Rev. E*65, 051913, 2002.

[4] J.L. Aragon, C. Varea, R.A. Barrio and P.K. Maini. Spatial patterning in modified Turing systems: Application to pigmentation patterns on marine fish. *Forma*, 13:213-221, 1998.

[5] M. Bani-Yaghoub and D.E. Amundsen. The role of Retinoic Acid and Notch in the symmetry breaking instabilities for axon formation. Presented at the *International Conference on Mathematical Biology, World Scientific and Engineering Academy and Society (WSEAS)*, Jan. 20, 2006, Miami, FL, USA.

[6] M. Bani-Yaghoub and D.E. Amundsen. Turing-type instabilities in a mathematical model of Notch and Retinoic Acid pathways. *WSEAS Transactions on Biology and Biomedicine*, 3(2):89-96, 2006.

[7] R.A. Barrio, C. Varea and J.L. Aragon. A two-dimensional numerical study of spatial pattern formation in interacting systems. *Bull. Math. Biol.*, 61:483-505, 1999.

[8] T.K. Callahan and E. Knobloch. Pattern formation in three-dimensional reaction-diffusion systems. *Physica D*, 132:339-362, 1999.

[9] J. Collier et al. Pattern formation by lateral inhibition with feedback: Mathematical model of Delta-Notch intercellular signaling. *J. Theor. Biol.*, 183:429-446, 1996.

[10] F.W. Cummings. A model of morphogenesis. *Physica A*, 339:531-547, 2004.

[11] A. De Wit. Spatial patterns and spatiotemporal dynamics in chemical systems. *Adv. Chem. Phys.*, 109:435-513, 1999.

[12] C.G. Dotti and G.A. Banker. The establishment of polarity by hippocampal neurons in culture. *J. Neurosci.*, 8:1454-1468, 1988.

[13] V. Castets, E. Dulos, J. Boissonade and P. DeKepper. Experimental evidence of a sustained standing Turing-type nonequilibrium chemical pattern. *Phys. Rev. Lett.*, 64:2953-2956, 1990.

[14] J.L. Franklin et al. Autonomous and non-autonomous regulation of mammalian neurite development by Notch1 and Delta1. *Current Biol.*, 9:1448-1457, 1999.

[15] A. Gierer and H. Meinhardt. A theory of biological pattern formation. *Kybernetik*, 12:30-39, 1972.

[16] P. Grindrod. *The Theory and Applications of Reaction-Diffusion Equations.*(Second Edition). Oxford University Press: Oxford, 1996.

[17] J. Hale and H. Kocak. *Dynamics and Bifurcations.* Springer-Verlag: New York, 1991.

[18] P. Hartman. *Ordinary Differential Equations.* John Wiley and Sons: New York, 1964.

[19] L.N. Howard and N. Kopell. Slowly varying waves and shock structures in reaction-diffusion equations. *Studies in Applied Mathematics*, 56:95-145, 1977.

[20] H. Ikeda. On the asymptotic solutions for a weakly coupled elliptic boundary value problem with a small parameter. *Hiroshima Math. J.*, 16:227-250, 1986.

[21] E.H. Kim. Singular Gierer-Meinhardt systems of elliptic boundary value problems. *J. Math. Anal. Appl.*, 308:1-10, 2005.

[22] E.H. Kim. A class of singular Gierer-Meinhardt systems of elliptic boundary value problems. *Nonlinear Anal.*, 59(3):305-318, 2004.

[23] N. Kopell and L.N. Howard. Plane wave solutions to reaction-diffusion equations. *Studies in Applied Mathematics.*, LII(4):291-328, 1973.

[24] T. Lepannen, M. Karttunen, K. Kaski, R.A. Barrio and L. Zhang. A new dimension to Turing patterns. *Physica D*, 168-169:35-44, 2002.

[25] J. Lewis. Notch signaling in control of cell fate choices in vertebrates. *Cell Dev. Biol.*, 9:583-589, 1998.

[26] C.S. Lin, W.M. Ni and I. Takagi. Large amplitude stationary solutions to a chemo-taxis system. *J. Differential Equations*, 72:127, 1988.

[27] M. Mimura, M. Tabata and Y. Hosono. Multiple solutions of two-point boundary value problems of Neumann type with a small parameter. *SIAM J. Math. Anal.*, 11(4):613-631, 1980.

[28] J.D. Murray, *Mathematical Biology I*, Springer-Verlag: New York, 2003.

[29] J.D. Murray, *Mathematical Biology II*, Springer-Verlag: New York, 2003.

[30] J.L. Napoli. Biochemical pathways of retinoid transport, metabolism, and signal transduction. *Clin. Immunology and Immunopathology*, 80(3):S52-S62, 1996.

[31] W.M. Ni. Diffusion, cross-diffusion, and their spike-layer steady states. *Notices Amer. Math. Soc.*, 45:918, 1998.

[32] Y. Nishiura and H. Fujii. Stability of singularly perturbed solutions to systems of reaction-diffusion equations. *SIAM J. Math. Anal.*, 18(6):1726-1770, 1987.

[33] T. Ohta, M. Mimura and R. Kobayashi. Higer-dimensional localized patterns in excitable media. *Physica D*, 34:115-144, 1989.

[34] M.R. Owen, J.A. Sherratt and S.R. Myers. How far can a juxtacrine signal travel? *Proc. R. Society*, 266:579-585, 1999.

[35] J.E. Pearson and W. Horsthemke. Turing instabilities with nearly equal diffusion coefficients, *J. Chem. Phys.*, 90:1588, 1989.

[36] J.J. Perraud, K. Agladze, E. Dulos and P. De Kepper. Stationary Turing patterns versus time-dependent structures in the chlorite-iodide malonic acid reaction, *Physica A*, 188:1-16, 1992.

[37] L. Perko. *Differential Equations and Dynamical Systems.* (Second Edition), Springer-Verlag: New York, 1996.

[38] E.M. Rauch and M.M. Millonas. The role of trans-membrane signal transduction in Turing-type cellular pattern formation. *J. Theor. Biol.*, 226:401-407, 2004.

[39] A.B. Rovinsky. Turing bifurcation and stationary patterns in the ferroin-catalyzed Belousov-Zhabotinskii reaction, *J. Phys. Chem.*, 91:4606, 1987.

[40] A. Rovinsky and M. Menzinger. Interaction of Turing and hopf bifurcations in chemical systems, *Phys. Rev. A*, 46(10):6313-6322, 1992.

[41] K. Sakamoto and H. Suzuki. Spherically symmetric internal layers for activator-inhibitor systems I. Existence by a LyapunovSchmidt reduction. *J. Differential Equations*, 204:56-92, 2004.

[42] K. Sakamoto and H. Suzuki. Spherically symmetric internal layers for activatorinhibitor systems II. Stability and symmetry breaking bifurcations. *J. Differential Equations*, 204:93-122, 2004.

[43] S. Sawai, Y. Maeda, and Y. Sawada. Spontaneous symmetry breaking Turing-type pattern formation in a confined dictyostelium cell mass. *Phys. Rev. Lett.*, 85:2212-2215, 2000.

[44] C.P. Schenk, M. Or-Guil, M. Bode and H.G. Purwins. Interacting pulses in three component reaction-diffusion systems on two-dimensional domains. *Phys. Rev. Lett.*, 78(19):3781-3784, 1997.

[45] J. Schnackenberg. Simple chemical reaction systems with limit cyclebehavior. *J. Theor. Biol.*, 81:389-400, 1979.

[46] M.E. Taylor. *Partial Differential Equations III.* Springer-Verlag:New York, Applied Mathematical Sciences, v.117, 1996.

[47] D. Thomas. Artificial enzyme membranes,transport, memory, and oscillatory phenomena. In D. Thomas and J.P. Kernevez, editors, *Analysis and Control of Immobilized Enzyme Systems*, pp.115-150. Springer-Verlag, Berlin-Heidelberg-New York, 1975.

[48] A.M. Turing, The chemical basis of morphogenesis, *Phils. Trans. Roy. Soc.* London Ser. B237, 37-72, 1952.

[49] H.J. Wearing, M.R Owen, and J.A. Sherratt. Mathematical modelling of juxtacrine patterning. *Bull. Mathematical Biol.*, 62:293-320, 2000.

[50] S.D. Webb and M.R. Owen. Intra-membrane ligand diffusion and cell shape modulate juxtacrine patterning. *J. Theor. Biol.*, 230:99-117, 2004.